Identification of Functional Regions of *Streptococcus agalactiae* CAMP Factor

by

TianHua Zhang

A thesis
presented to the University of Waterloo
in fulfillment of the
thesis requirement for the degree of
Master of Science
in
Chemistry

Waterloo, Ontario, Canada, 2008

I hereby declare that I am the sole author of this thesis. This is the true copy of the thesis, including any required final revisions, as accepter by my examiners.

I understand that my thesis maybe made electronically available to the public.

TianHua Zhang

Abstract

Streptococcus agalactiae CAMP factor is a protein exotoxin that contains 226 amino acid residues and forms oligomeric pores on susceptible cell membranes and liposomes. In this study, fragments of CAMP factor were created and recombinantly expressed to identify functional domains that are involved in membrane binding, oligomerization, and membrane insertion. Altogether, six truncated forms of CAMP factor were created and assayed. $CAMP^{1-113}$, $CAMP^{1-170}$, $CAMP^{57-226}$, and $CAMP^{171-226}$ showed different levels of hemolytic activity. $CAMP^{1-56}$ and $CAMP^{114-226}$ did not show hemolytic activity or oligomerization ability, but showed binding ability. $CAMP^{114-226}$ inhibited the hemolytic activity of wild-type CAMP factor, most likely through 'one-sided' oligomerization. From the comparison of these fragments, it emerges that the region between residues 57 and 113 plays a crucial role in oligomerization and membrane insertion. The high binding efficiency of $CAMP^{114-226}$ suggests this region has great responsibility on membrane binding. The hemolytically inactive fragments showed higher binding efficiency than some of the active fragments. For the hemolytic fragments, higher binding efficiency gave stronger hemolysis. These findings support that CAMP factor has different functional regions for pore-formation.

Acknowledgements

I would like to thank my supervisor, Dr. Michael Palmer, for giving me the opportunity to work in his laboratory. I really appreciate his unreserved support and patience through the project.

I would like to thank my advisory committee members, Dr. Elizabeth Meiering and Dr. Thorsten Dieckmann for their helpful suggestions and comments.

I would like to thank my lab mates, Dr. Shenhui Lang, Lisa Pokrajac, Dr. Waseem El-Huneidi, David Donkor, Eric Brefo-Mensah, Muhammad Khan, Muhammad Salah, and Jawad Muraih for their help and support.

I would like to thank my wonderful friends in the department: Dr. Nicole Sukdeo, Dr. Zhengding Su, Dr. Jessica Rumfeldt, Uthaiwan Suttisansanee, Cullen Myers, Ronald Zahorulk, Ignace Moya, Meijun Lu, Kadia Mullings, Zlatko Lejic, Allen Chu, Tingxi Ying, Odi Israel, Yay Duangkhan, Opeyemi Jeje, Gracie Hwang, and Ming Tong, for their help and all the great time spend together.

Particularly, I would like to extends my appreciations to my great frinds: Pei Chun Hang, Jason Da Costa, Dr. Nicole Sukdeo, Danish Khan, Zijian Long, Xu Jin, Martin Smith, Jen Kurz, and Scott Bonilla for their invaluable friendship, help and comfortable guest rooms.

To my family

Table of Contents

List of Figures

List of Tables

List of Abbreviations

Å	Ångstrøm
BSA	Bovine serum albumin
DTT	Dithiothreitol
E. coli	*Escherichia coli*
EDTA	Ethylene diaminotetraacetic acid
F109C	Phenylalanine substituted with cysteine at position 109
GPI	Glycosylposphatidylinositol
HEPES	N-2-Hydroxyethylpiparazine-N'-2-Ethanesulfonic acid
IPTG	Isopropyl-1-thio-β-D-galactopyranoside
kDa	Kilo-Dalton
LB	Luria Bertani broth
Leukocidin F	LukF
MDT	Membrane-damaging toxin
PBS	phosphate-buffered saline
PCR	Polymerase chain reaction
PEG	Polyethylene glycol
PFO	perfringolysin O
PFT	Pore-forming toxin
S. agalactiae	*Streptococcus agalactiae*
S. aureus	*Staphylococcus aureus*
SDS-PAGE	Sodium dodecyl sulfate polyacrylamide gel electrophoresis
SLO	Streptolysin O
TMH	Transmenbrane helices

Chapter 1 Introduction

Membranes define the boundary of the basic biological unit, the cell. They also compartmentalize the various subcellular organelles, such as nuclei, chloroplasts, and mitochondria, in eukaryotes. Membranes function as the protective barriers for the cells. They are also involved in regulating the trafficking of materials between different organelles within cells and also the trafficking of materials between cells. The damage on membranes may lead to cell lysis and death. For defensive purpose, certain organisms create toxins to damage the membanes of their invaders. Some organisms create toxins damaging target membranes to facilitate their growth and reproduction.

1.1 Membrane-Damaging Proteins and Peptides

Membrane-damaging proteins and peptides are represented in a range of organisms including humans, bacteria, insects, fungi, amoeba, and plants. They are classified into three groups according to their different membrane-damaging mechanisms: enzymatic toxins, detergent-like toxins, and pore-forming toxins.

1.1.1 Enzymatic toxins

Enzymatic toxins damage the membranes by enzymatically hydrolyzing the phospholipids that constitute the cell membrane bilayers (Figure 1.1). The subsequent physical changes might finally lead to the collapse of the membrane [*1*]. Enzymatic toxins exhibit phospholipase activity, such as the *Clostridium perfringens* α-toxin (phospholipase C) and *Vibrio damsela* hemolysin (phospholipase D). Some of them exhibit sphingomyelinase activity, such as *Staphylococcus aureus* β-toxin [*2, 3*].

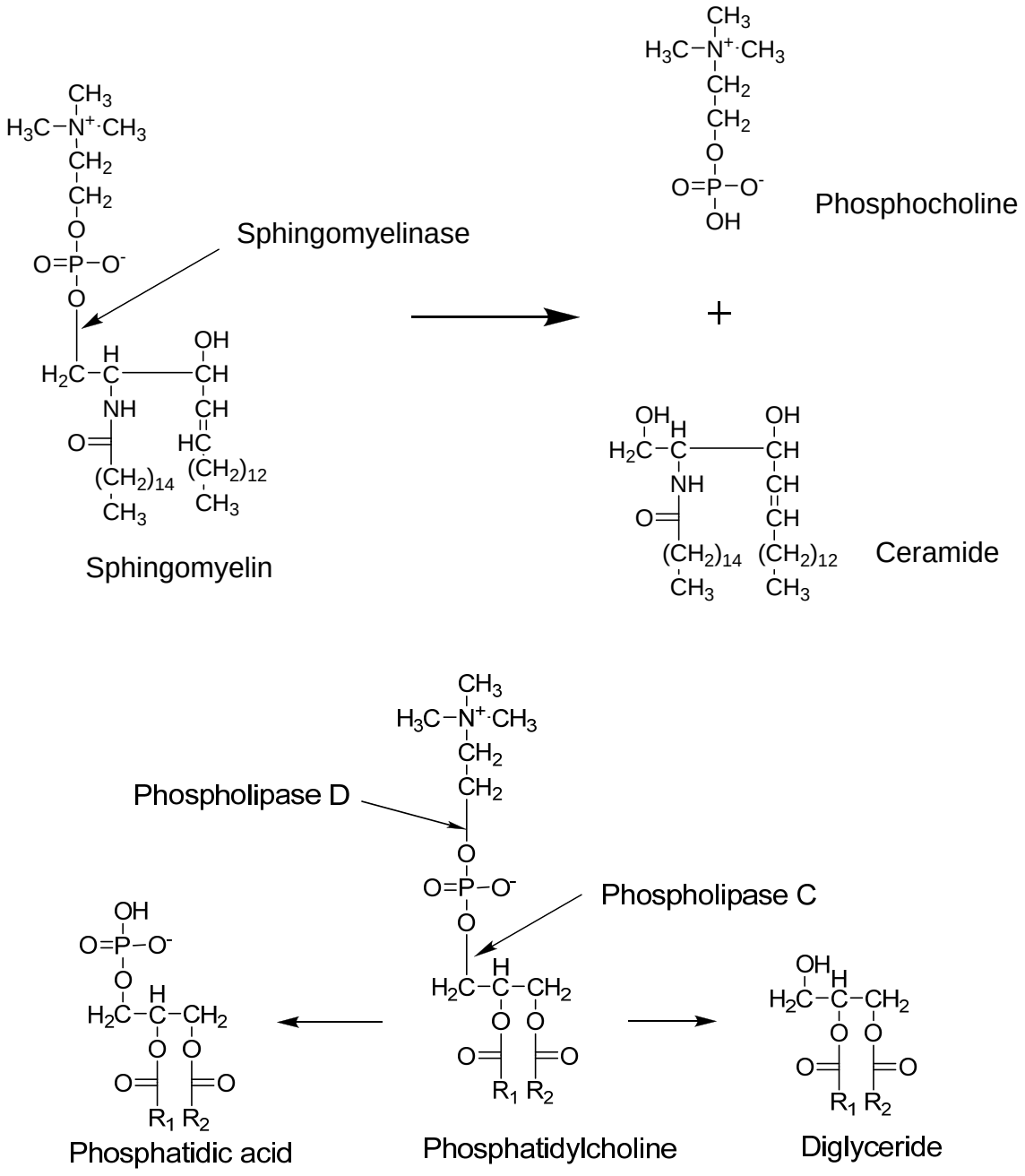

Figure 1. 1: The reactions catalyzed by sphingomyelinase and phospholipase C and D.

1.1.2 Detergent-like toxins

These toxins permeabilize the membrane by a detergent-like (surfactant) activity that results in membrane solubilization or partial insertion of the toxin into the hydrophobic cores of target membranes, such as *Staphylococcus aureus* δ-toxin [*4*]. They are usually α-helical shaped or would adopt helical structure in the membrane-bound state [*5, 6*].

Two models of membrane disruption have been proposed for these toxins: the "carpet" model and the "barrel-stave" model (Figure 1.2). In the "carpet" model, the lytic peptides bind to the target membrane surface and cover it like a carpet, inserting in between the phospholipid head groups. When a threshold concentration has been reached, the resulting strain on the lipid packing results in temporary membrane permeation and finally disintegration of the membrane into micelles. In the "barrel-stave" model, the amphipathic α-helices of the toxin insert into the membrane and recruit more monomers to from transmembrane channels/pores [*7*].

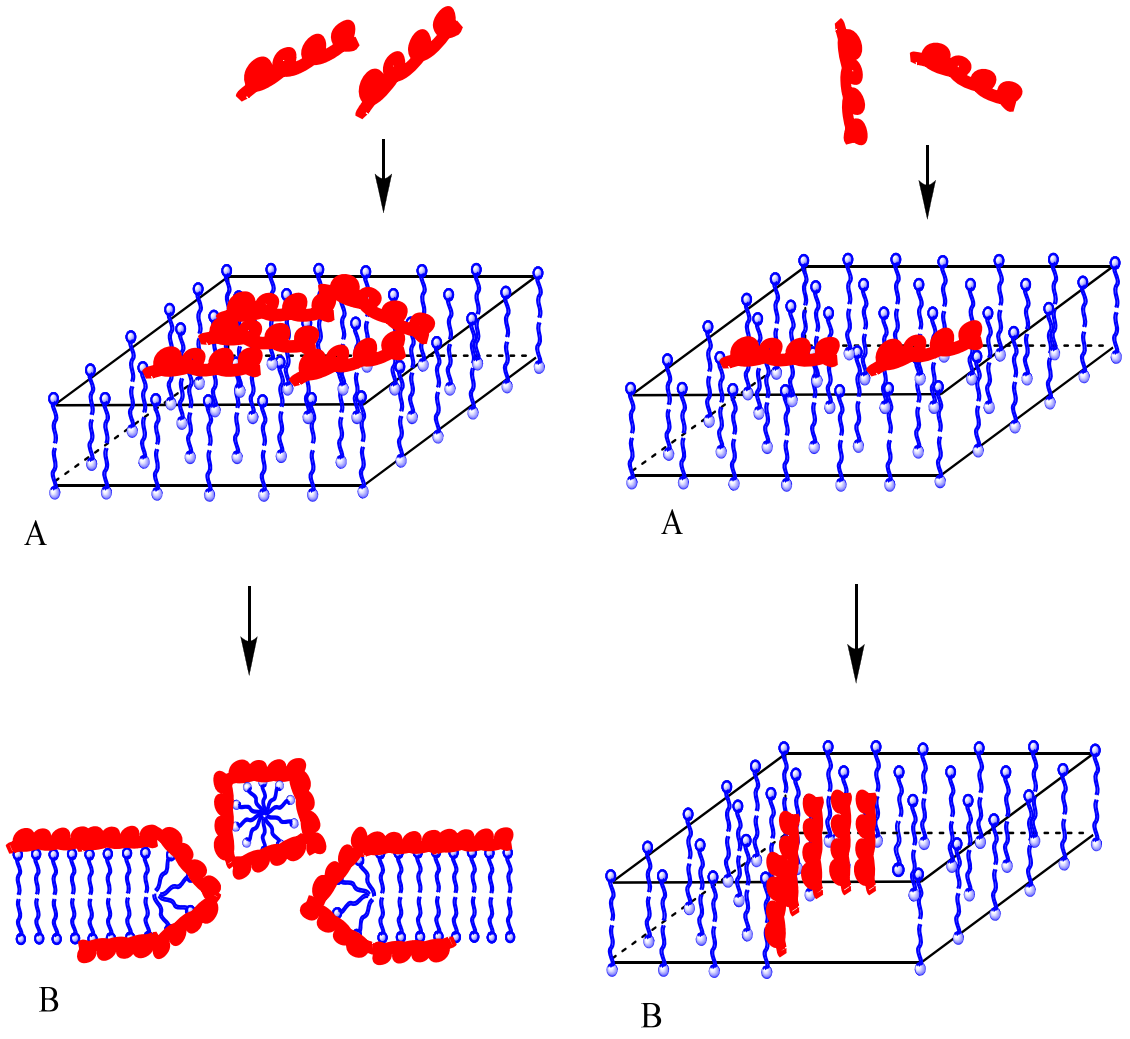

Figure 1. 2: The "carpet" (to the left) and "barrel-stave" (to the right) models of membrane permeation by lytic-peptides.

In the "carpet" model, the amphipathic peptides bind to the membrane surface with their hydrophobic sides and expose their hydrophilic sides to the solvent thereby distending the head group layer of the membrane (step A). When a threshold concentration has been reached, the ensuing membrane curvature strain leads to the disruption of membrane continuity and the formation of transient pores and micelles (B). In the `barrel-stave' model, the amphipathic peptides first assemble in the surface of the membrane (A), then insert into the lipid core of the membrane following recruitment of additional monomers. Their hydrophobic sides interact with the core of the membrane lipids, and their hydrophilic sides face the aqueous pore (B) [*7*].

1.1.3 Pore-forming toxins

This group comprises the majority of the membrane-damaging proteins and peptides. They are produced by a number of organisms, such as bacteria, plants, fungi, primitive metazoans, insects and humans [*8*] (Table 1.1). CAMP factor is also from this group.

Table 1. 1 Examples of pore-forming proteins and peptides.

Origin	Target	Examples
Man	Bacteria	Complement [*9*]
Man	Man	Complement [*9*]
Bacteria	Man	*Streptococcus agalactiae* CAMP factor [*10, 11*]
Bacteria	Bacteria	Colicins [*2*]
Bacteria	Insects	*Bacillus thuringiensis* toxins [*12, 13*]
Insects	Bacteria	Cecropin [*14, 15*]
Insects	Man	Melittin [*16*]
Ameoba	Bacteria	Amoebapore [*17*]
Fungi	Bacteria	Alamethicin [*18*]

1.1.3.1 The general mechanism of pore-forming toxins (PFTs)

The toxins are produced and released primarily as water soluble monomeric proteins which bind to the target cell membranes [*1*]. The binding of PFTs to membranes usually occurs via specific receptors, such as cholesterol and glycosylphosphatidylinositol (GPI)-anchored proteins [*19-22*]. The membrane bound PFTs oligomerize and from a pre-pore complex, which undergoes significant conformational change that leads to the insertion of the oligomer into the lipid matrix. Concomitantly, the hydrophobic surfaces of the toxin proteins are exposed to the lipids and a transmembrane pore is formed that is lined by

hydrophilic residues (Figure 1.3). These pores vary in size, from 1-2nm with *S aureus* α-toxin [*23-25*], to 25-30nm in perfringolysin O [*26, 27*]. Both ring- and arc-shaped pores have been observed by electron microscopy [*23, 24*].

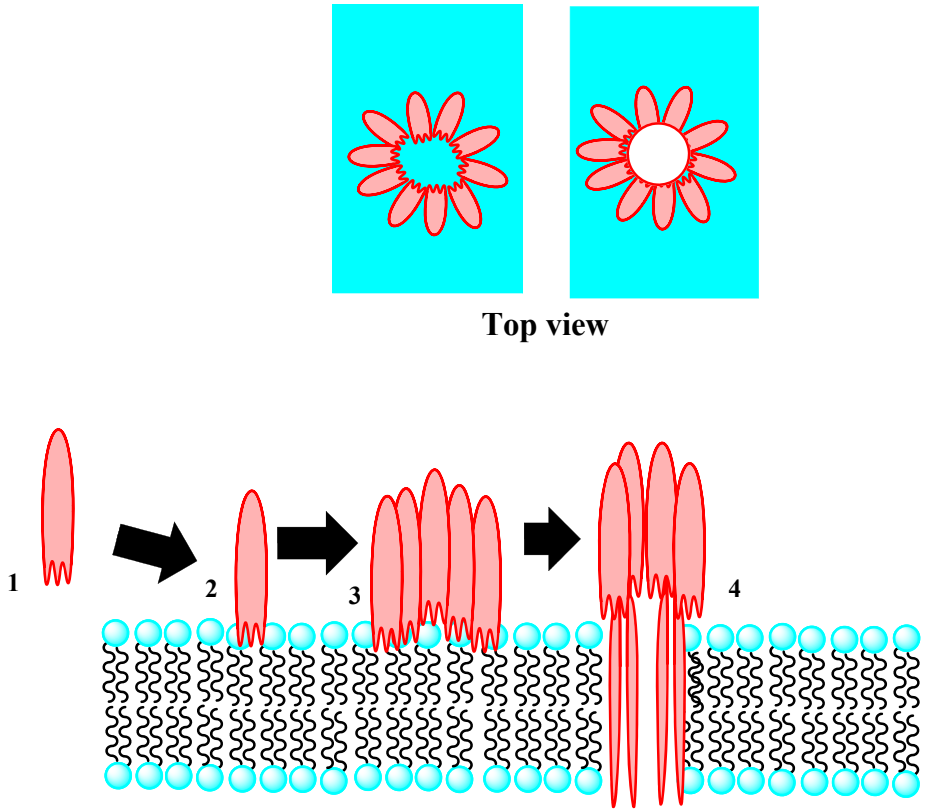

Figure 1. 3: The general mechanism of pore formation.

Toxins are released as water-soluble monomers (1), bind to membrane, often via specific receptors (2), oligomerize with other membrane bound toxins and form the pre-pore complex (3), the complex undergoes conformational changes, and inserts into the membrane and forms a pore (4) [*25*].

1.1.4 Biological function of PFTs

PFTs are secreted by various bacteria to disrupt and damage the host cell membranes. For some non-pathogenic bacteria, such as *Bacillus alvei* and *Bacillus cereus*, they help to maintain their saprophytic life style [*20*]. For pathogenic bacteria, these toxins are important as virulence factors, which contribute to bacterial survival and spread in the host organisms. Many invasive bacteria when rendered unable to produce their PFTs exhibit reduced or abolished virulence [*28-31*]. During infection of host organisms, pore formation causes osmotic imbalance that consequently leads to cell swelling, lysis, and death [*2*]. Lysis of the white blood cells may reduce the host's antibacterial immune response and promote the spread of bacteria. The transmembrane pore also provides access to essential intracellular nutrients to facilitate bacterial growth and reproduction [*32*].

1.1.5 Prototypical PFTs

PFTs exist in two distinct stable states. Initially, they are water-soluble and monomereic; after membrane binding, they undergo a significant conformational change that converts them to the oligomeric membrane-inserted and lipophilic form [*33, 34*]. While the three-dimentional structure of the monomeric forms of several PTFs are known, only very few oligomer structures have been solved by crystallography or characterized in sufficient details with other means. The following sections describe well-studied PFTs that are used as structural models for other less characterized toxins.

1.1.5.1 *Staphylococcus aureus* α-hemolysin

α-hemolysin is released by *Staphylococcus aureus* as a 33 kDa water-soluble monomer which forms a heptameric β-barrel transmembrane pore on the surface of susceptible cells, leading to cell lysis and death. There is only the heptamer crystal structure of α-hemolysin solved, and only the monomer structure for leukocidin F (LukF) (Figure 1.4) [*24, 35*]. However, both toxins are sufficiently similar for us to consider the two crystal structures as complementary models of a common monomer and oligomer structure [*36*]. LukF is very similar in structure with the α-hemolysin monomer when it is situated within the heptamer pore (Figure 1.4B, C), except for the stem domains and the "amino latch" structure [*37*]. In the LukF, the amino latch is packed closely towards its β-sandwich core, whereas in the α-hemolysin, it reaches to its adjacent protomer and forms a strong contact. The stem domain is folded in close proximity to the β-sandwich core to maintain the monomer's water solubility. In the heptamer, the stem domain is unfolded and it inserts into the membrane with one β-hairpin. The amino latch has an extended conformation when the monomer converts to the pore-forming conformation.

The complete four-step performing process of α-hemolysin is based upon the two previously described structures:

1. α-hemolysin is secreted by S *aureus* as a water-soluble monomer with its stem domain folded.
2. The toxin monomers move towards host cells and bind to their membranes without significant conformational change.

3. The bound monomers oligomerize to each other with the N-terminal amino latch. Engaging in key inter-monomer interaction. A non-lytic heptamer is formed on the cell surface.
4. The pre-stem domains from the non-lytic heptamer unfold and insert into the membrane. Each monomer contributes one β-hairpin, which lines the transmembrane portion of the channel. The membrane-inserted form of the heptamer is mushroom shaped, with a 100Å in diameter and height, and a 26Å channel diameter.

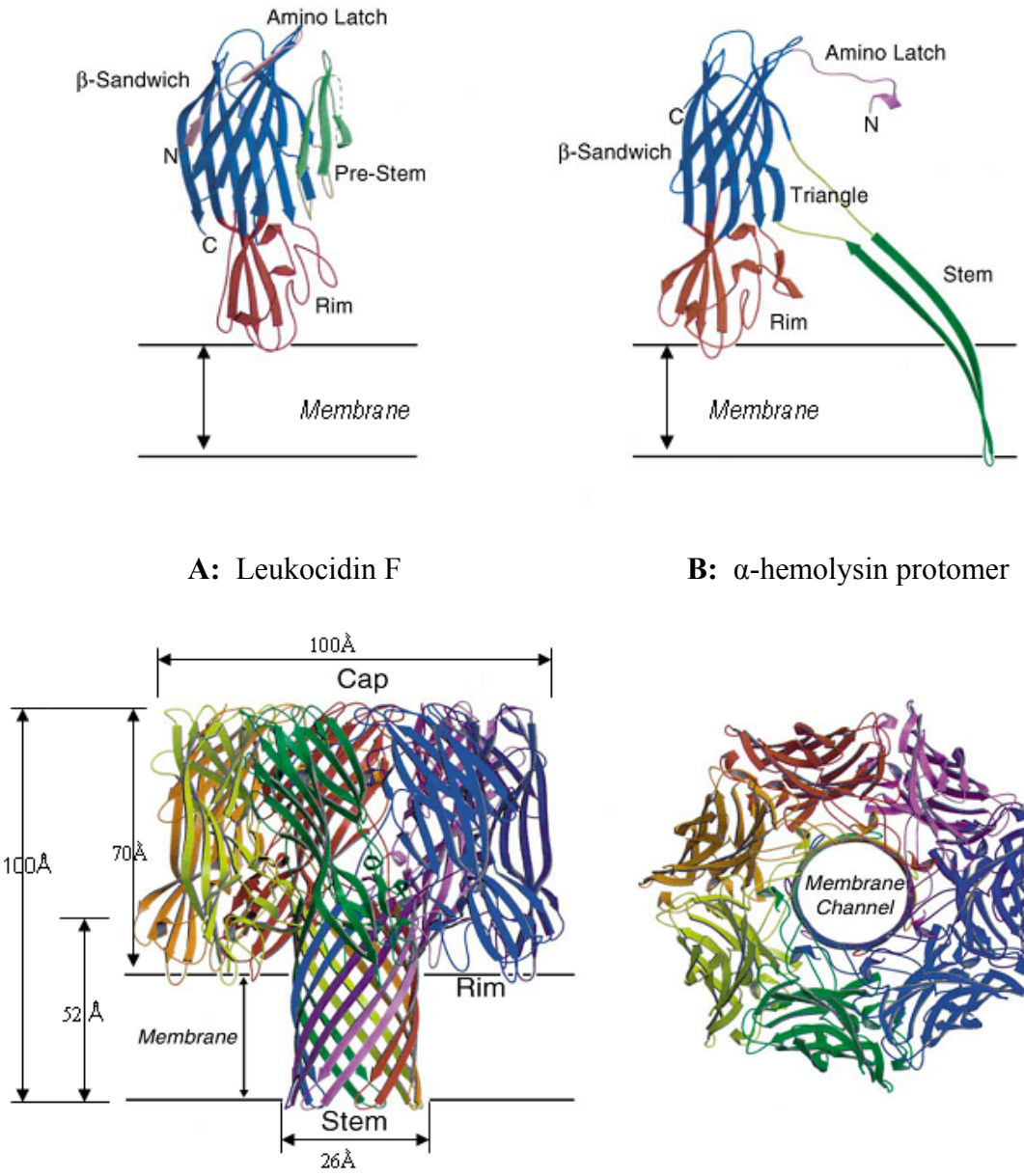

A: Leukocidin F

B: α-hemolysin protomer

C: α-hemolysin heptamer side view

D: Top view of heptamer

Figure 1. 4: Ribbon representation of Leukocidin F and α-hemolysin.

Leukocidin F monomer (A), the α-hemolysin protomer of its membrane inserted heptamer (B), the side view (C), and top view (D) of α-hemolysin heptamer [*36, 37*].

1.1.5.2 Cholesterol-Dependent Cytolysins

Cholesterol-Dependent Cytolysins (CDCs) constitute the largest family PFTs, and they are also one of the most common bacterial toxins [*2, 19, 38*]. They exhibit some unique features:

1. Their cytolytic activity shows an absolute dependence on the presence of the cholesterol in the membrane.
2. They form very large oligomeric complexes containing up to 50 monomers and the resulting transmembrane pore can be up to 300Å in diameter.
3. Many mutagenesis and spectroscopic studies have suggested that in the water-soluble monomeric form their pre-stem domains are folded into short α-helices. These helices are thought to convert to long transmembrane β-hairpins that insert into the membrane.

Streptolysin O (SLO) and perfringolysin O (PFO) are the two most extensively characterized CDCs with respect to structure and function. The crystal structure of the monomeric, water-soluble PFO has been determined (Figure 1.5) [*27*], but there is no structure available for any CDC membrane-inserted oligomer yet. There are four domains in PFO as shown in Figure 1.5. In the water-soluble monomeric form, there are two transmembrane helices (TMHs) in domain 3. During the pore formation, these two α-helices change their conformation to two β-hairpins that insert into the cell membrane [*27, 39-42*].

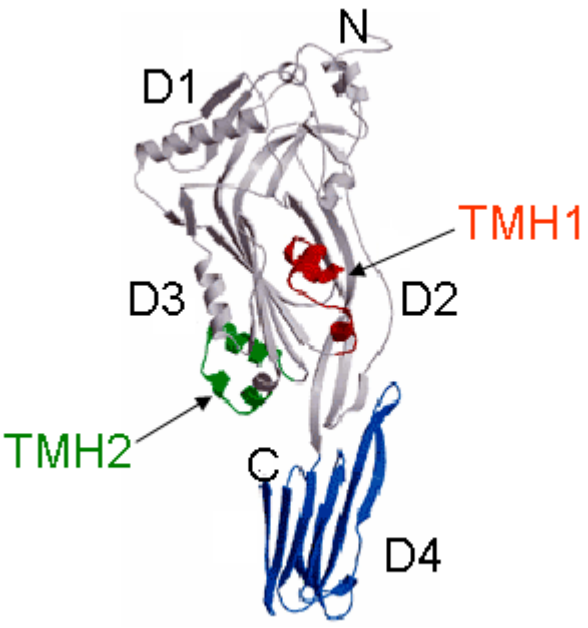

Figure 1. 5: Ribbon representation of water-soluble form of PFO.
Domains 1-4 are denoted (D1-D4) on the Figure. The location of TMH1 and TMH2 are colored in red and green, respectively.

1.2 CAMP factor

CAMP factor is an extracellular protein toxin secreted by several *Streptococcus* species, such as *Streptococcus agalactiae* (*S. agalactiae*). *S. agalactiae* CAMP factor has 226 amino acid with a mass of 25 kDa [*43*]. It is the toxin studied in this project.

1.2.1 CAMP reaction

CAMP factor derives its name from the CAMP reaction, which was first described in 1944 by Christie, Atkins, and Munch-Petersen. The term CAMP reaction was initially applied only to the synergistic hemolytic reactions between *S. aureus* and group B streptococci [*44*]. During the last few years, this term has also been used to describe the

synergistic lysis of red blood cells in the presence of exosubstances produced by microorganisms growing adjacent to each other on the surface of blood agar [*45*].

The CAMP reaction has been widely used as a diagnostic method to identify *S. agalactiae*. The nutrient sheep agar plate is used in this procedure. *S. aureus*, which produces sphigomyelinase, and the putative strains of *S agalactiae* are streaked across the plate at right angles, close but not touching each other. After incubation, if CAMP factor was produced by the strain, a distinct hemolytic zone would develop in the adjoining area of the two streaks (Figure 1.6) [*46-48*].

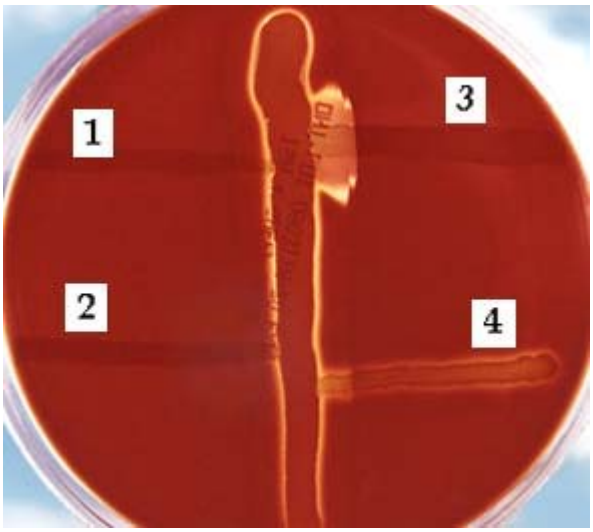

Figure 1. 6: A blood agar plate used in CAMP reaction after incubation at 37^{o}C for 24 hours.

The vertical streak is sphingomyelinase-producing *S aureus* strain. Strain 1, *Enterococcus faecalis*; Strain 2, *Streptococcus salivarius*; Strain 3, *S agalactiae*; Strain 4, *Enterococcus durans* [*48*].

1.2.2 Characterization of CAMP factor

Despite the wide application of the CAMP reaction for decades, little was know about the structure and function of CAMP factor. CAMP factor has no enzymatic activity to change membrane content [*43*]. It causes lysis of sphingomyelinase-treated red blood cells that contain at least 45mol% of sphingomyelin in the cell membrane, such as those of sheep (50mol%) and bovine (45mol%) erythrocytes [*10, 44, 49*]. Erythrocytes containing less than 30mol% sphingomyelin such as those of human (27mol%) and rabbit (19mol%) are not susceptible to CAMP factor lysis after sphingomyelinase treatment. However, these cells may become susceptible to CAMP factor after treatment with phospholipase C [*50, 51*]. Sphingomyelinase and phospholipase C convert sphingomyelin and phosphatidylcholine to ceramide and diacylglycerol, respectively (Figure 1.1). Therefore ceramide is not specifically required for the CAMP reaction. In contrast, cholesterol content in the membrane was shown to be critical for CAMP factor activity [*11, 51*].

Using electron microscopy (EM) and polyethylene glycol (PEG) osmotic protection studies, Lang and Palmer showed that CAMP factor formed pores on sphingomyelinase treated sheep erythrocytes [*11*]. Both regular round and irregular shaped pores were observed, and they varied in sizes, some of them with radii up to 12 nm [*11*]. The PEG protection experiments suggested that the hydrodynamic radius of these pores was between 1.6nm and 2.7nm [*11*]. Receptors on the membrane have been shown to be important for the surface recognition and pore-formation, such as cholesterol for CDCs and glycosylphosphatidylinositol (GPI)-anchored proteins for aerolysin [*1*]. CAMP factor is known to bind to GPI-anchored proteins [*22*].

1.2.3 CAMP factor as virulence factor

Neutralizing antibodies against CAMP factor were found in the sera of group B *Streptococcus* (GBS)-inoculated rabbits and cows [*52*]. CAMP factor was not found to be lethal to mice, but mice developed fatal septicaemia after injection with sub-lethal dose of GBS and repeated doses of purified CAMP factor [*53, 54*].

CAMP factor was called protein B in some studies because it was reported to bind to the Fc arms of immunoglobulin (Ig) G and IgM [*53*]. Recent studies suggested that CAMP factor could not bind to human IgG [*55*].

1.3 Research objectives

According to the previous studies, the pore-forming process of CAMP factor was suggested to be highly cooperative and to follow the general mechanism of PFTs [*11, 56*]. The objective of this project is to identify the functional regions which are responsible for *S. agalactiae* CAMP factor binding, oligomerization, and membrane insertion during the pore-forming process. The general strategy for characterization is to create truncated forms of CAMP factor by site-directed mutagenesis. These CAMP factor fragments were characterized using biochemical assays for haemolytic activity, membrane binding, and oligomerization.

Chapter 2 Experimental procedures

2.1 Reagents and equipments

Primers, glutathione-agarose resin, glutathione, thrombin from human plasma, sphingomyelinase, bovine serum albumin (BSA) were purchased from Sigma-Aldrich (Oakville, ON). Dimethyl sulfoxide (DMSO) was from Caledon (Georgetown, ON), Glycerol was from EMD chemicals (Gibbstown, NJ). Fluorescein-5-maleide was bought from Biotium (Burlington, ON). Polyethylene glycol (PEG) 3500 was from Fluka (Germany). *Escherichia coli* (*E. coli*) XL1 Blue cells were from Clontech (Palo Alto, CA), E. coli BL21 (DE3) cells were from Novagen (Madison, WI). All lipids were from Avanti Lipids (Alabaster, AL). Amplex Red cholesterol assay kit was from Invitrogen (Eugene, OR) Ampicillin, kanamycin and the rest of the chemicals were bought from Bioshop (Burlington, ON). Sheep red blood cells (citrated) were from Cedarlane Laboratories (Hornway ON). Deoxynucleoside triphosphates (dNTP) and Expanded High Fidelity PCR Kit were from Roche (Indianapolis, IN). Thrombin protease was purchased from Amercham Biosciences (Uppsala, Sweden). DNA markers, protein marker, and Restriction endonucleases (REs) ApaI, EcoRI, PsiI, SspI were purchased from MBI fermentas (Burlington, ON). P6DG gel was from BioRad (Richmond, CA). Nickel-nitrolotriacetic acid (Ni-NTA) resin and QIAprep spin miniprep kit were from Qiagen (Mississauga, ON). Superdex 75 (HR10/30) column was from Amersham (Piscataway, NJ).

BioRad-Biological LP high performance liquid chromatography (HPLC) system (CA), Techne TC-512 PCR system (Techne cambridge, UK), Spectramax-190 96-well plate reader (Molecular Devices, Sunnyvale, CA), Micromass Q-Tof Ultima GLOBAL mass

spectrometer (Waters, MA), emulsifier EmulsiFlex-C5 (Avestin), liposome extruder (Northern Lipids, Vancouver, BC) and QuantaMaster 4 fluorimeter (Proton technology Inc. London, ON) were used.

2.2 Mutagenesis

2.2.1 Plasmid

Plasmid pET 30 a(+) with cloned methionine-free CAMP factor (CAMP M21L M107L) was used as the mutagenesis template. A DNA sequence for a 6X His-tag and thrombin cleavage site are located at the N terminus of the CAMP factor encoding gene.

2.2.2 Recombination-based polymerase chain reaction (PCR)

The mutagenesis procedure was based on the method developed by Howorka and Bailey where amino acid substitutions are introduced by polymerase chain reaction (PCR)[*57*]. In each PCR mutagenesis, four primers were used, including a pair of non-mutagenic primers (pGEX*fwd* and pGEX*rev*) and a pair of mutagenic primers with 12 overlapped base pairs. A single cysteine substitution was introduced here as well. The primer design is schematically represented in Figure 2.1.

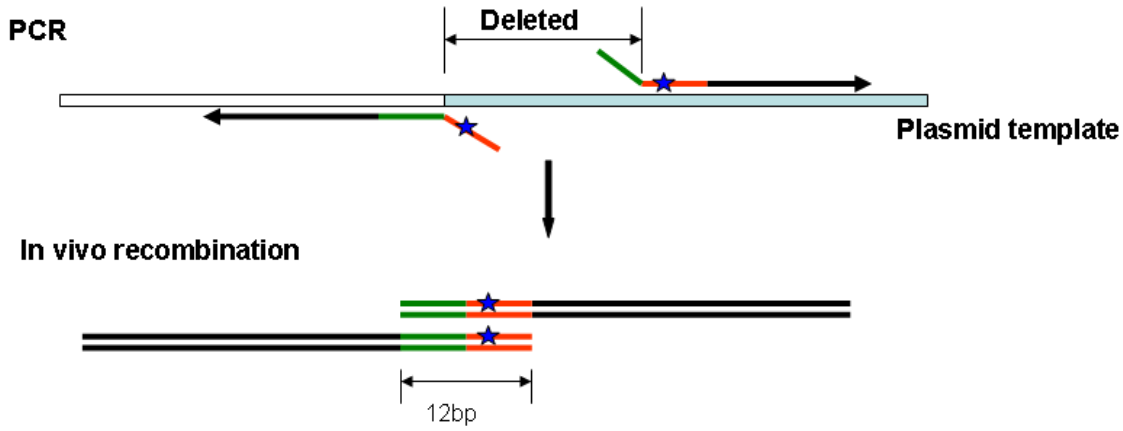

Figure 2. 1: Mutagenic primer design:

Each pair of the mutagenic primers has 12 overlapped base pairs (bp), shown in green and red. For each primer, there are 18 bases complementary to the plasmid template, shown as parallel to the template. The cysteine substitution (blue star) is introduced into the overlapped CAMP factor region (red). After *in vivo* recombination, specific parts of the CAMP factor gene would be deleted. There were 6 pairs of mutagenic primers designed as shown in Table 2.1.

Initially, the template plasmid was linearized in separate digests with different restriction enzymes (REs). It was linearized with EcoRI for pGEX*rev* and forward mutagenic primer. SspI was used to other linearization. Secondly, the corresponding primers were used the PCR amplification (Table 2.2, and 2.3)). Then the PCR products were mixed and transformed into *Escherichia coli* XL-1 Blue competent cells (Figure 2.2).

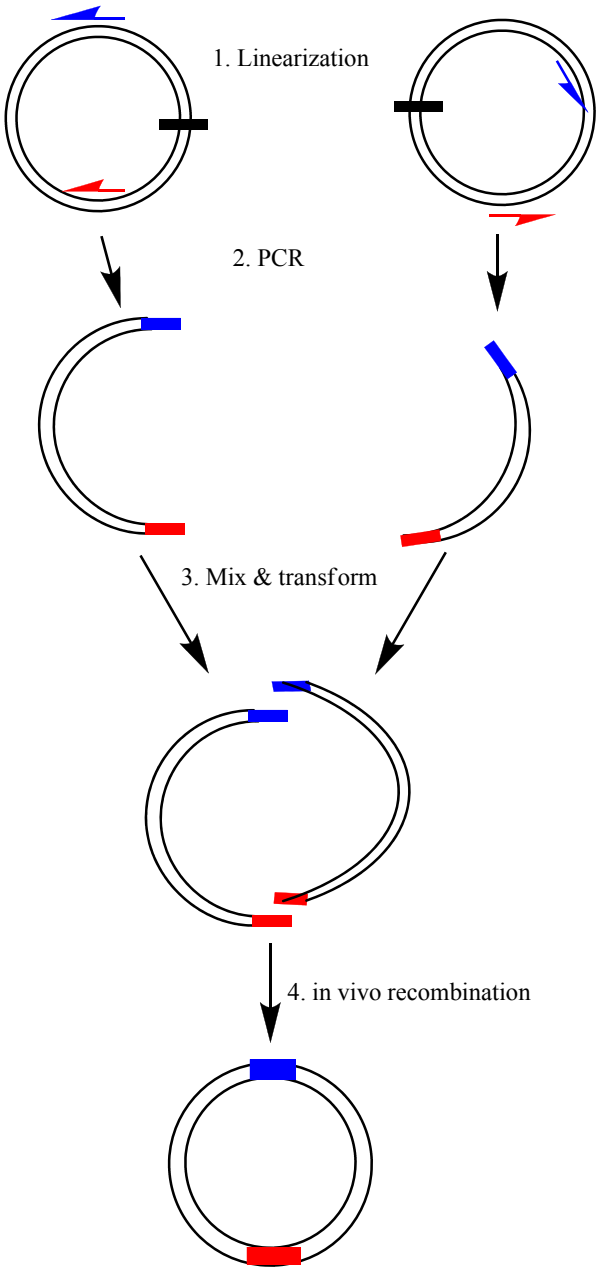

Figure 2. 2 Schematic representation of recombination-based PCR mutagenesis:
The non-mutagenic and mutagenic primer pairs are shown in red and blue, respectively. 1, the template plasmid is linearized separately using different restriction enzymes. 2, PCR. After the PCR, only the gene encoding the desired CAMP factor fragment would be amplified. 3, PCR products are mixed and transformed into XL-1 blue cells. Then the plasmid with CAMP factor fraction gene would be obtained after in vivo recombination [*57*].

Table 2. 1: CAMP factor fragmentation and Non-mutagenic primers (pGEX*fwd* and pGEX*rev*) primers.

CAMP$^{1\text{-}113}$	
CAMP$^{1\text{-}113}$*fwd*	5' TTTGCCCTAGTTATTTGCATTTTAG 3'
CAMP$^{1\text{-}113}$*rev*	5' AACTAGGGCAAAATCAGCCATGGC 3'
CAMP$^{114\text{-}226}$	
CAMP$^{114\text{-}226}$*fwd*	5' ACTAAGTAATATTTGTATTTGTATTTTTCG 3'
CAMP$^{114\text{-}226}$*rev*	5' ATATTACTTAGTTATCCCACATCCCAG 3'
CAMP$^{1\text{-}56}$	
CAMP$^{1\text{-}56}$*fwd*	5' GTTGAATAATATTTGTATTTTTCG 3'
CAMP$^{1\text{-}56}$*rev*	5' ATATTATTCAACGCAAGTAATAGC 3'
CAMP$^{57\text{-}226}$	
CAMP$^{57\text{-}226}$*fwd*	5' TCTGGTAAATTAAAGACTTGCTTG 3'
CAMP$^{57\text{-}226}$*rev*	5' TAATTTACCAGAACCGCGTGGCAC 3'
CAMP$^{1\text{-}170}$	
CAMP$^{1\text{-}170}$*fwd*	5' TGTACATAATATTTGTATTTTTCG 3'
CAMP$^{1\text{-}170}$*rev*	5' ATATTATGTACACCAAATTTCCTTATC 3'
CAMP$^{171\text{-}226}$	
CAMP$^{171\text{-}226}$*fwd*	5' TCTGGTTGTTTTACTAGAGATAAAAAAG 3'
CAMP$^{171\text{-}226}$*rev*	5' AAAACAACCAGAACCGCGTGGCAC 3'
Non-mutagenic primers	
pGEX*fwd*	5' AAGACGATAGTTACCGGATAAG 3'
pGEX*rev*	5' AAGACGATAGTTACCGGATAAGGC 3'

Table 2. 2: Reagents used in the PCR.

Deionized, autoclaved water	40 µL
Linearized template plasmid DNA	1 µL (~ 1 µg)
pGEX*fwd*/ pGEX*rev*	1 µL (300nM, final)
Reversed/ forward mutagenic primer	1 µL (300nM, final)
dNTP	1 µL (200 µM, final)
10X PCR buffer with $MgCl_2$(15mM)	5 µL
Expand high fidelity DNA polymerase mixture	1 µL
Total	50 µL

The mixtures were transferred into PCR tubes, vortexed and centrifuged briefly. The PCR were performed in a Techgene thermal cycle (Techne, Cambridge, UK) under the following conditions:

Table 2. 3: PCR conditions.

Pre-heating	95^{o}C	3 minutes
Number of cycles	25	
Melting	95^{o}C	30 seconds
Annealing	See Table 2.4	30 seconds
Extension	72^{o}C	75 seconds
	End of the cycle	
Final extension	72^{o}C	10 minutes

Table 2. 4: Annealing temperatures for different PCRs.

pGEX*rev*/ CAMP$^{1\text{-}113}$*fwd*, pGEX*fwd*/ CAMP$^{1\text{-}113}$*rev*, pGEX*rev*/ CAMP$^{57\text{-}226}$*fwd*	50^{o}C
pGEX*rev*/ CAMP$^{114\text{-}226}$*fwd*, pGEX*fwd*/ CAMP$^{114\text{-}226}$*rev*, pGEX*fwd*/ CAMP$^{1\text{-}170}$*rev*	52.5^{o}C
pGEX*fwd*/ CAMP$^{57\text{-}226}$*rev*, pGEX*rev*/ CAMP$^{1\text{-}170}$*fwd*	55.4^{o}C
pGEX*rev*/ CAMP$^{1\text{-}56}$*fwd*, pGEX*fwd*/ CAMP$^{1\text{-}56}$*rev*, pGEX*rev*/ CAMP$^{57\text{-}226}$*fwd*, pGEX*fwd*/ CAMP$^{57\text{-}226}$*rev*	57.4^{o}C

The PCR products were analyzed by agarose gel electrophoresis for purity and size. The matching DNA fragments were mixed and transformed into XL-1 Blue competent cells.

2.2.3 Plasmid extraction and verification

Positive colonies were selected from LB agar plates containing kanamycin (20μg/mL) to inoculate 3 ml of sterilized LB media containing kanamycin (20μg/ml) and grown overnight with shaking (200 rpm) at 37 ^{o}C. The plasmid was extracted from this culture using QIAprep Spin Miniprep Kit. The plasmid was digested with PsiI and ApaI to confirm its size by agarose gel electrophoretic analysis. The plasmid with desired size was sent for sequencing at University of Waterloo (Molecular Biology Core Facility) to ensure that the correct mutation had been introduced. The plasmid was transformed into *E. coli* BL21 (DE3) cells for expression.

2.3 Preparation of competent cells and transformation

2.3.1 Preparation of *E. coli* XL-1 Blue heat-shock competent cells and heat-shock transformation

1 ml of fresh overnight XL-1 Blue cell culture was diluted into 100 ml of sterilized LB broth and grown at 37^{o}C with vigorous shaking to reach an optical density (OD600) of 0.4. The cells were harvested at 3000 revolutions per minute (rpm) for 15 minutes at 4^{o}C. The supernatant was discarded and the cell pellet was resuspended in 1 ml LB and 1 ml 2X transformation and storage buffer (20 %(w/v) PEG 3350, 10% (v/v) dimethyl sulfoxide, 50%(V/V) LB medium, 100mM $MgCl_2$, pH6.5) on ice. These cells were aliquoted (100 μL) and stored at -80^{o}C [*58*].

For the transformation, 1 μL of PCR product was added to one aliquot of thawed cells and incubated on ice for 30 minutes. The cells were heat shocked by placing the tube in a 42 ^{o}C water bath for 45 seconds and then cooled on ice for 3 minutes. Then the cells were transferred into 1 ml of SOC media and grown at 37^{o}C with vigorous shaking for 1 hour. 100 μL of the SOC culture was spread on LB agar plate with 20 μg/ml kanamycin.

2.3.2 Preparation of *E. coli* BL21 (DE3) electroporation competent cells and transformation

5 ml of fresh overnight BL21 (DE3) cell culture was diluted into 500 ml of sterilized LB broth and grown at 37^{o}C with vigorous shaking to reach an OD600 of 0.6. The cells were collected by centrifugation at 3000 rpm for 15 minutes at 4^{o}C. The supernatant was discarded and the cell pellet was resuspended in 500 ml of ice-cold 10% glycerol. The cells were harvested again following centrifugation and resuspended in 250 ml of ice-cold 10% glycerol. The cells were concentrated one more time by centrifugation and re-suspension in

2 ml of ice-cold 10% glycerol.The suspension was aliquoted (40 μL) and stored at -80^{o}C [*59*].

0.4 mL of plasmid DNA was added to one aliquot of thawed cells and electroporated in a BioRad cell pulser electroporation unit. Then the cells were transferred into 1 ml of SOC media (0.5% (w/v) yeast extract, 2% (m/v) tryptone, 10 mM NaCl, 2.5 mM KCl, 10 mM $MgCl_2$, 20mM $MgSO_4$, 20 mM glucose), and grown at 37^{o}C with vigorous shaking for 1 hour. 100 μL of the SOC culture was spread on LB agar plate with 20 μg/ml kanamycin.

2.4 Expression and purification of CAMP factor and its fragments

Both CAMP factor and its fragments were expressed in *E. coli* BL21 (DE3) cells. A single colony with the plasmid of interest was picked and inoculated into 20 ml of Luria Bertani (LB) media containing antibiotics (100μg/ml ampicillin for CAMP factor, 20μg/ml kanamycin for mutants), and grown overnight at 37 ^{o}C with shaking (200 rpm). The overnight culture was diluted into 1 liter of LB media containing appropriate antibiotics, and grown at 30^{o}C with vigorous shaking until the OD_{600nm} reached 0.8. The protein expression was induced by adding isopropyl-1-thio-β-D-galactopyranoside (IPTG) to a final concentration of 1 mM. The cells were grown for an additional 4 hours at 37^{o}C and harvested by centrifugation at 3000 rpm at 4 ^{o}C for 15minutes and stored at -20 ^{o}C overnight.

For CAMP factor, the cell pellet was thawed on ice and resuspended in 15ml of phosphate-buffered saline (PBS) (16mM K_2HPO4, 150 Mm NaCl, pH 7.2) containing protease inhibitor mixture (Sigma). For $CAMP^{1-113}$, $CAMP^{114-226}$, $CAMP^{1-56}$, and $CAMP^{1-170}$, the cell pellets were resuspended in low concentration imidazole buffer (50 mM Tris,

250 mM NaCl, 50 mM imidazole, pH 7.5). For $CAMP^{57-226}$ and $CAMP^{171-226}$, the cell pellets were resuspended in lysis buffer (100mM NaH_2PO_4, 10 mM Tris, 6M guanidine hydrochloride, 10 mM imidazole, pH8). The cells were lysed by using an emulsifier at 17000 psi. The lysates were centrifuged at 20000rpm for 15 minutes at 4°C, and the supernatants were used for the purification. All the purifications were performed at 4°C.

CAMP factor fragments were purified using a Ni-NTA affinity column (5mL) and BioRad-Biological LP HPLC system were used for their purification. For $CAMP^{1-113}$, $CAMP^{114-226}$, $CAMP^{1-56}$, and $CAMP^{1-170}$, the lysates were injected to the column pre-equilibrated with low concentration imidazole buffer. The column was washed with 10 volumes of low imidazole buffer; the protein was eluted in gradient with high concentration imidazole buffer (50 mM Tris, 250 mM NaCl, 250 mM imidazole, pH7.5). For $CAMP^{57-226}$ and $CAMP^{171-226}$, the lysates were injected into the column pre-equilibrated with lysis buffer. The column was washed with 10 volumn buffer A (100 mM NaH_2PO_4, 150 mM NaCl, 8 M urea, 20 mM imidazole, pH8) followed by 10 volume buffer B (50 mM NaH_2PO_4, 500 mM NaCl, 20 mM imidazole, pH8) and eluted in elution buffer (50 mM NaH_2PO_4, 500 mM NaCl, 250 mM imidazole pH7.5). These proteins were desalted using P6DG column pre-equilibrated with thrombin cleavage buffer (50 mM Tris, 150 mM NaCl, 2.5 mM $CaCl_2$, pH8.0). Thrombin was added to the protein solutions to a final concentration of 6 μg/ml and incubated for 30 minutes at room temperature. Then the protein solutions were run through P6DG column pre-equilibrated with Tris buffer (50 mM Tris, 150 mM NaCl, 1 mM EDTA, 5 mM DTT, pH7.5), CAMP factor fragments were collected and stored at -80°C with 10%(V/V) glycerol. The protein concentrations were determined by the Bradford method using bovine serum albumin (BSA) as a standard [*60*].

CAMP factor was expressed as a glutathione-S-transferase fusion protein[*11*]. The purification method used was published by Guan and Dixon[*61*]. Briefly, the supernatant was run through a 5 ml glutathione-agarose column for 3 cycles. The column was washed with 10 volumes of PBST buffer (PBS buffer with 1% Triton X100), 4 volumes of PBS buffer and followed by 4 column volumes of thrombin cleavage buffer (50mM Tris, 150mM NaCl, 2.5 mM $CaCl_2$, pH 8) at room temperature. The column was suspended in 2 ml of thrombin buffer containing 12 μg of thrombin and shaken gently at room temperature for 1 hour. The protein was eluted with thrombin cleavage buffer and stored at -80^{o}C with 10% (V/V) glycerol.

2.5 Protein labelling

Cysteine is a very strong nucleophile in a protein and also very rare in a protein, which makes it easily to be modified by a variety of reagents, such as maleimide. Maleimide reacts with the sulfhydryl group of cysteine with very high specificity, and its derivatives have been used to modify the cysteine residues in many proteins[*62*]. By combining site-specific mutagenesis and cysteine modification techniques, the cysteine-free CAMP factor can be labelled by cysteine modification.

The cysteine-substituted CAMP factor or CAMP factor fragments were exchanged into labelling buffer (50 mM Tris, 150 mM NaCl, 1 mM EDTA, pH7.5) with P6DG column at room temperature. A 10-fold molar excess of dye (fluorescein maleimde, or rhodamine maleimde) was dissolved in 10 μL of DMSO. 500 μL of the protein was added to the dye and incubated in the dark at room temperature for 45 minutes. The unbound dye was removed by P6DG column with labelling buffer as eluant.

2.6 Hemolytic assay

400 μL of sheep red blood cells were washed 5 times in HEPES buffer (20 mM HEPES, 150 mM NaCl, pH 7.4) by centrifugation at 2000 rpm for 4 minutes. The cells were resuspended in HEPES buffer to 0.5% (V/V). The cell suspension was incubated with 10 mM $MgCl_2$ and 50 milliunits/mL *S. aureus* sphingomyelinase (Sigma) at 37^{o}C for 5 minutes. Serial two-fold dilutions of CAMP factor and its fragments were prepared in microtiter plate in 20 μL of HEPES buffer. Then 180 μL of the sphingomyelinase-treated cells were added. Haemolytic activity was measured by the decrease in turbidity (OD_{650nm}) using a 96-well plate reader over a period of 60 minutes at room temperature.

2.7 Binding of CAMP factor fragments to erythrocyte membranes and chemical cross-linking

The protein sample was added into the sphingomyelinase-treated ghost membranes, and incubated at 37^{o}C for 45 minutes. The membranes were spun down at 13000 rpm for 10 minutes and unbound proteins in the supernatant were discarded as supernatant. The membranes were resuspended and washed with Tris buffer (50mM Tris, 150 mM NaCl, pH7.5) by centrifugation for 3 times. The membrane pellet was dissolved in Tris buffer containing 10% (w/v) sodium deoxycholate. The dissolved membranes were analyzed by 15% sodium dodecyl sulphate polyacrylamide gel electrophoresis (SDS-PAGE) to estimate the binding ability of the protein.

Protein samples were incubated with liposomes (total lipids: 0.2 mg/ml) in HEPES buffer at 37^{o}C for 30 minutes. The cross-linking reagent glutaraldehyde was added to 2.5 mM and incubated for another 30 minutes. The reaction was stopped by adding 1M Tris; to 0.1 M. Then the sample was analyzed for protein binding by 10% SDS-PAGE.

2.8 Hemolytic inhibition of CAMP factor fragments to CAMP factor

The cell preparation was the same as the one described in section 2.5. Serial two-fold dilutions of CAMP factor fragments were prepared in a microtiter plate in 15 μL of HEPES buffer, 5 μL of diluted CAMP factor was added into each of them. Then 180 μL of cells were added, and the haemolytic activities were measured.

2.9 Membrane binding competition of CAMP factor fragments to CAMP factor

Except the possibility of being inhibited during oligomerization (described in section 2.8), hemolysis could also be inhibited through competition for membrane binding receptors. Therefore, fragments that showed hemolytic inhibition would also have to be assayed for inhibition of CAMP factor binding.

The ghost membranes were prepared as described in section 2.10. CAMP factor mutant (F109C) was labelled with fluorescein maleimide as described in section 2.5. Serial two-fold dilutions of CAMP factor fragments were prepared in microcentrifuge tubes in 30 μL of HEPES buffer. To each dilution, 10 μL of diluted labelled CAMP factor F109C was added into each of them. Then 360 μL of membranes were added and incubated at 37 ^{o}C for 20 minutes. The membranes were spun down at 13000 rpm for 10 minutes and unbound proteins in the supernatant were discarded. The membranes were resuspended and washed with HEPES buffer by centrifugation at 13000 rpm for 10 minutes for 3 times. The membranes were dissolved in Tris buffer with 1% SDS, and the fluorescein fluorescence intensity was measured as described in section 2.13.

2.10 Preparation of erythrocyte ghost membranes

400 μL of sheep red blood cells were osmotically lysed in 5 mM phosphate buffer (pH7.2), and the membrane were pelleted and washed by centrifugation at 13000 rpm for 10 minutes. The washing was repeated several times until the membrane appeared white. The membranes were resuspended in HEPES buffer with 10 mM $MgCl_2$. Then they was incubated with 50 milliunits/mL sphingomyelinase for 20 minutes at 37^{o}C

2.11 Preparation of liposomes

Ceramide, cholesterol, and phosphatidylcholine were dissolved in 1 mL of chloroform at molar ratio of 40:45:15 to a final lipid concentration of 2 mg/ mL. The mixture was dried to a thin film under nitrogen gas in a round-bottom flask and dried for additional 3 hours under vacuum. The lipids were hydrated at 45^{o}C for 1 hour with HEPES buffer. The suspension was frozen at -20^{o}C and thawed at 45^{o}C, and then extruded through polycarbonate membranes with 100 nm pore size using a liposome extruder at 45 ^{o}C to form unilamellar liposomes. The extrution was repeated 20 times. The final lipid concentration was determined by using Amplex Red Cholesterol Assay Kit.

2.12 Gel filtration

A Superdex-75 gel filtration column (HR10/30) was equilibrated with Tris buffer (50mM Tris, 150 mM NaCl, pH7.5). The protein sample was exchanged to the same Tris buffer using P6DG column, applied to Superdex-75 column and eluted with same buffer.

2.13 Spectrofluorimetry

Fluorescein-labelled protein was incubated with sphygomyelinase-treated ghost membranes and washed as described in section 2.10 but dissolved in Tris buffer containing 1% (W/V) SDS. A membrane suspension without protein was used as blank. The fluorescence emission intensity was measured between 500 nm and 600 nm after excitation at 492 nm.

2.14 Mass spectrometry

A Micromass Q-Tof Ultima GLOBAL mass spectrometer was used for protein analysis by positive ion electrospray ionization mass spectrometry. The protein was exchanged into water using a P6DG column and mixed with acetonitrile/ water solution (0.2% formic acid) in a ratio of 1:1. The final protein concentration is approximately 5 μM. The data was processed using MaxEnt1 (Waters, MA) to generate the molecular mass spectra.

Chapter 3 Results and Discussion

3.1 Construction of CAMP factor fragments

All together, six fragments of CAMP factor were constructed: $CAMP^{1-113}$, $CAMP^{114-226}$, $CAMP^{1-56}$, $CAMP^{57-226}$, $CAMP^{1-170}$, and $CAMP^{171-226}$ (Figure 3.1).

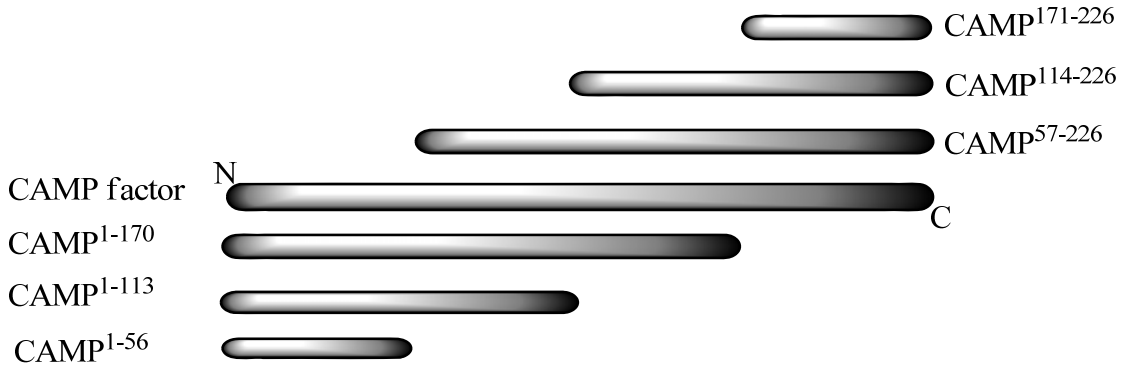

Figure 3. 1: Schematic representation of the fragments with wild type CAMP factor.

The primers were designed based on plasmid pET30 a(+) encoding His-tagged CAMP factor. To obtain the optimal PCR products, different annealing temperatures were tested in small PCR mixture volume (5 μL in total). The PCR products generated by primer pair pGEX*rev*/ $CAMP^{1-56}$*fwd* with different annealing temperatures were analyzed by 1% agarose gel electrophoresis shown as an example in Figure 3.1. The purest PCR product (Lane 4) was produced with annealing temperature was 57.4^{o}C. Then the full scale (50μL) PCR was performed and used for transformation. All other PCRs were analyzed and with the same method.

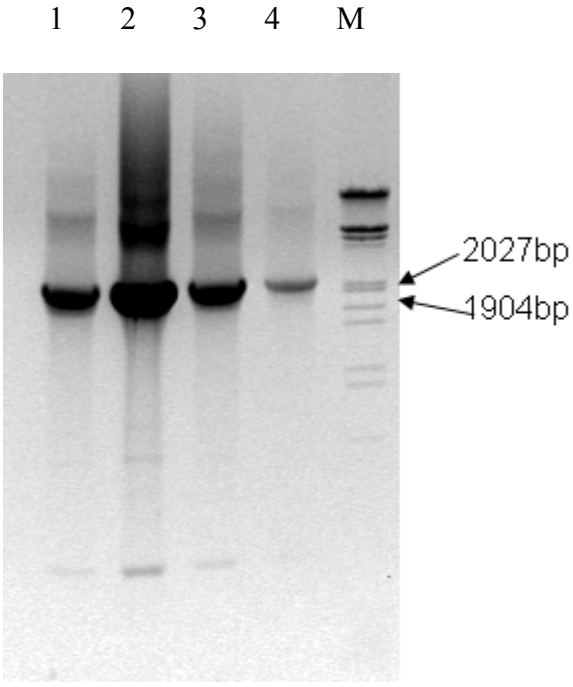

Figure 3. 2: PCR products from primer pair pGEX*rev*/ CAMP$^{1\text{-}56}$*fwd* with different annealing temperatures:
Lane1, 50^{o}C; Lane 2, 52.5 ^{o}C; Lane 3, 55.4 ^{o}C; Lane 4, 57.4 ^{o}C. Lane M: Lambda DNA/EcoRI+HindIII Marker.

After the PCR products were obtained, they were transformed into *E.coli* XL-1 Blue cells for *in vivo* recombination. Approximately 10 colonies were observed on each plate after 24 hours. Three colonies for each mutant were picked and grown for plasmid extraction. The plasmids were double digested by PsiI and ApaI, which gave two DNA fragments. The template CAMP factor plasmid was also double digested for comparison. Since specific regions of the gene were deleted, the lengths of the DNA fragments should be reduced accordingly. The DNA fragments were analyzed by 1% agarose gel electrophoresis. Analyses for CAMP$^{1\text{-}56}$ and CAMP$^{57\text{-}226}$ plasmids are shown as examples

in Table 3.1 and Figure 3.3. The plasmids confirmed by RE digestion analyses were also confirmed by sequencing.

Table 3. 1: The fragment lengths for template CAMP factor, $CAMP^{1-56}$, and $CAMP^{57-226}$ plasmids after double digestion by PsiI and ApaI.

Plasmid	Fragment length (bp)	Deleted length (bp)
Template CAMP factor plasmid	3765, 2250	---
$CAMP^{1-56}$ plasmid	3765, 1740	510
$CAMP^{57-226}$ plasmid	3765, 2082	168

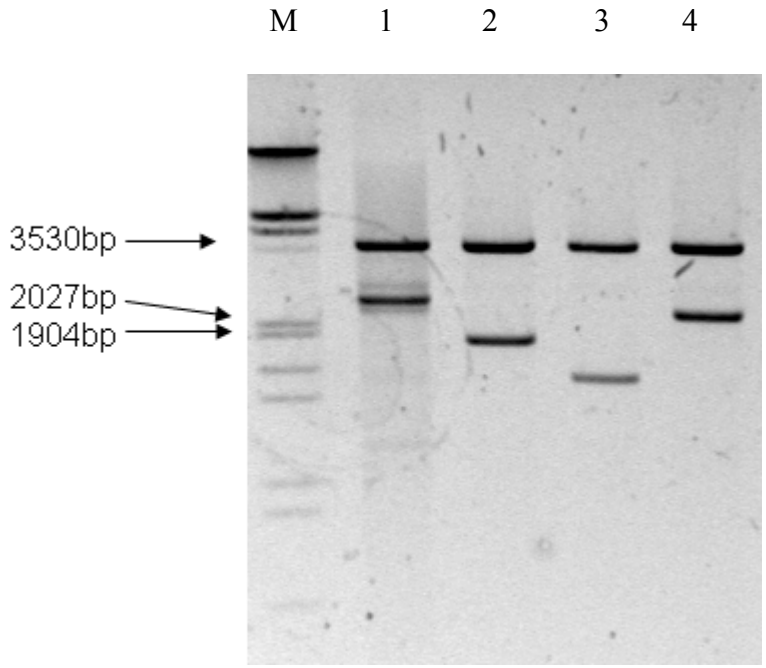

Figure 3. 3: Double digestion of plasmids.

Lane M, Lambda DNA/EcoRI+HindIII Marker; Lane 1, template CAMP factor plasmid; Lane 2, $CAMP^{1-56}$ plasmid; Lane 3, plasmid without desired mutation; Lane 4, $CAMP^{57-226}$ plasmid.

3.2 Expression and Purification of CAMP factor fragments

During the growth of cell cultures, cell samples were collected before IPTG induction and harvest; these samples were analyzed by SDS-PAGE to evaluate the protein expression.

All the CAMP factor fragments were expressed with His-Tag affixed. For the purification of $CAMP^{1-113}$, $CAMP^{114-226}$, $CAMP^{1-56}$, and $CAMP^{1-170}$, these His-tagged proteins bound to the Ni-NTA affinity column were eluted by increasing imidazole concentration above 200 mM. They were collected and cleaved with thrombin. The CAMP factor fragments were obtained after the His-tag was separated by P6DG gel filtration. CAMP 1-113 is shown as an example in Figure 3.4.

For the purification of $CAMP^{57-226}$ and $CAMP^{171-226}$, the same purification method as above was tried; however, there was only a very small amount of proteins were eluted from the column and they were not pure. The denatured purification method was tried, this protocol was expected to refold the protein on the column before the elution; however the protein was eluted in buffer A, which has very low imidazole concentration and was not expected to elute the proteins. Therefore, the protocol was modifid such that washing was done with imidazole-free buffer, followed by elution with buffer A.

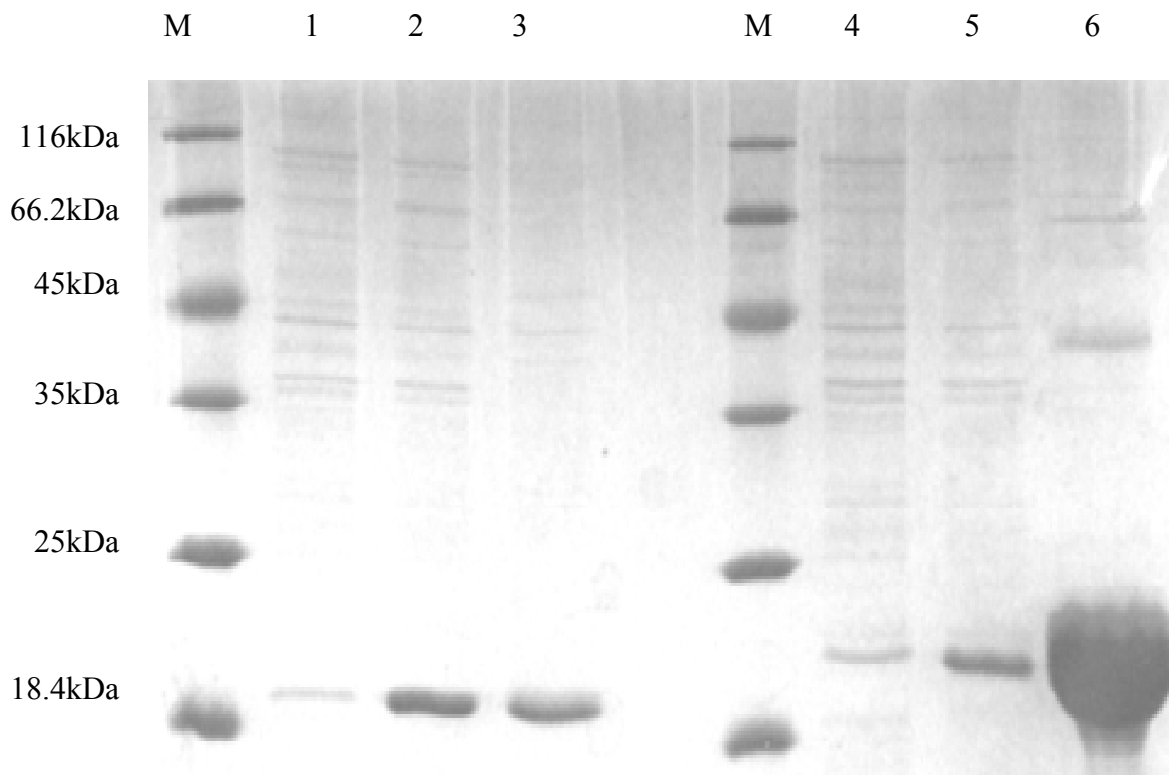

Figure 3. 4: Expression and purification of CAMP$^{1-113}$ in *E. coli* BL21 (DE3) analyzed by 15% SDS-PAGE.

Lane M, protein marker; Lane 1, 2 and 3, thrombin-cleaved protein after P6DG gel filtration. Lane 4 and 5, *E. coli* protein extract before and after IPTG induction, respectively; Lane 6, protein eluted from Ni-NTA column.

3.3 Hemolytic activity of CAMP factor fragments

Hemolytic activity assays were performed on all the six mutant fragments. $CAMP^{1-113}$, $CAMP^{57-226}$, $CAMP^{1-170}$, and $CAMP^{171-226}$ all showed activity, but much weaker comparing to intact CAMP factor. $CAMP^{1-56}$ and $CAMP^{114-226}$ did not show hemolytic activity (Figure 3.5).

For $CAMP^{1-113}$, 50% hemolysis was achieved in 30 minutes with a concentration of 400 μg/ml, comparing to CAMP factor achieved it in 15 minutes with a concentration of 1 μg/ml (Figure 3.5 A). $CAMP^{57-226}$ and $CAMP^{1-170}$ could achieve 50% hemolysis in 15 minutes at the concentrations of 12.5 μg/mL and 100 μg/mL, respectively. Within a longer period of time, these fragments lysed all the cells. $CAMP^{171-226}$ showed hemolytic activity but could not lyse all the cells; 50% hemolysis was achieved by $CAMP^{171-226}$ with a concentration of 400 μg/mL in 10 minutes, but lysis then did not progress any further (Appendix 1).

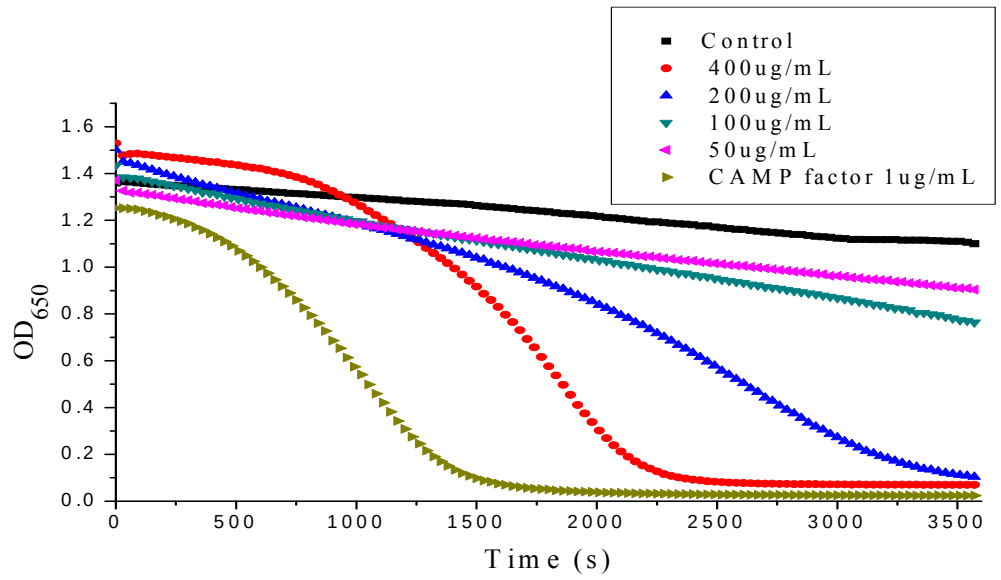

(A) CAMP$^{1-113}$

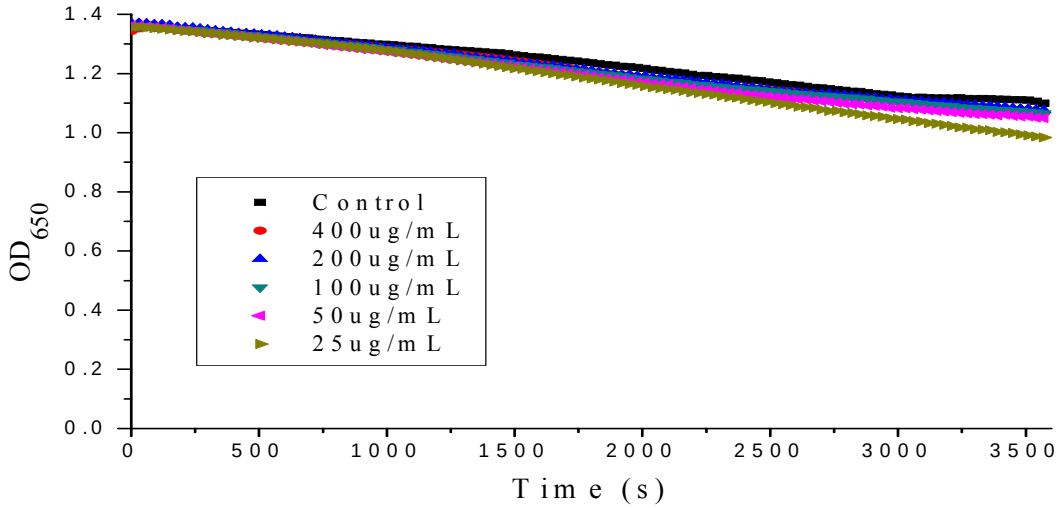

(B) CAMP$^{114-226}$

Figure 3.5: Hemolytic titration of CAMP factor and fragments.

Sheep red blood cells (0.5% (v/v), final) were treated with sphingomyelinase prior to the assay. Blood cells with no CAMP protein added were used as control. Hemolysis was assayed by the decrease in turbidity (OD_{650nm}) for one hour with a time interval of 30 second. (A) Hemolysis by CAMP$^{1-113}$ at different concentrations. CAMP factor at 1 µg/mL is shown for comparison. (B) Hemolysis by CAMP$^{114-226}$ at different concentrations.

3.4 Membrane binding of CAMP factor fragments

Since the pore-formation is a cooperative process that includes binding, oligomerization, and insertion, the loss of pore formation activity could be the consequence of the failure of any of the three steps.

Since $CAMP^{114-226}$ and $CAMP^{1-56}$ did not show hemolytic activity, they were tested for their ability to bind to cell membranes. These fragments were incubated with sphingomyelinase-treated sheep erythrocyte membranes, and then the membranes were analyzed by SDS-PAGE after being washed and dissolved. $CAMP^{114-226}$ showed binding to the membrane (Figure 3.6 A). The binding of $CAMP^{1-113}$ was also assayed to compare with $CAMP^{114-226}$, however, binding was very weak even with increased concentration.

$CAMP^{1-170}$ and $CAMP^{57-226}$ showed hemolytic activity, they were tested for binding ability as well (Figure 3.6 B). Although they showed same level of hemolytic activity, $CAMP^{57-226}$ showed much stronger binding ability comparing to $CAMP^{1-170}$.

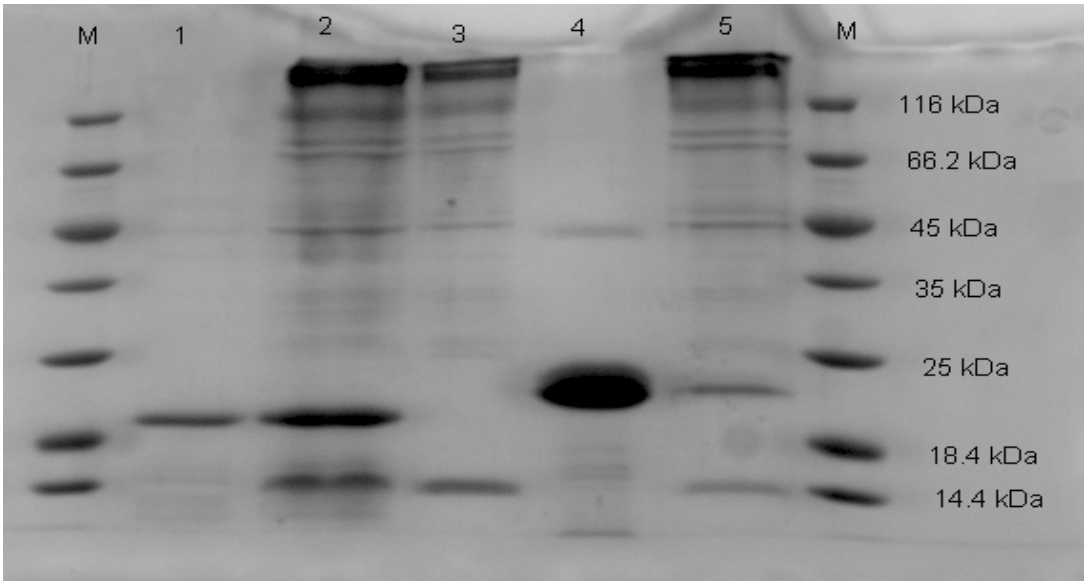

(A)

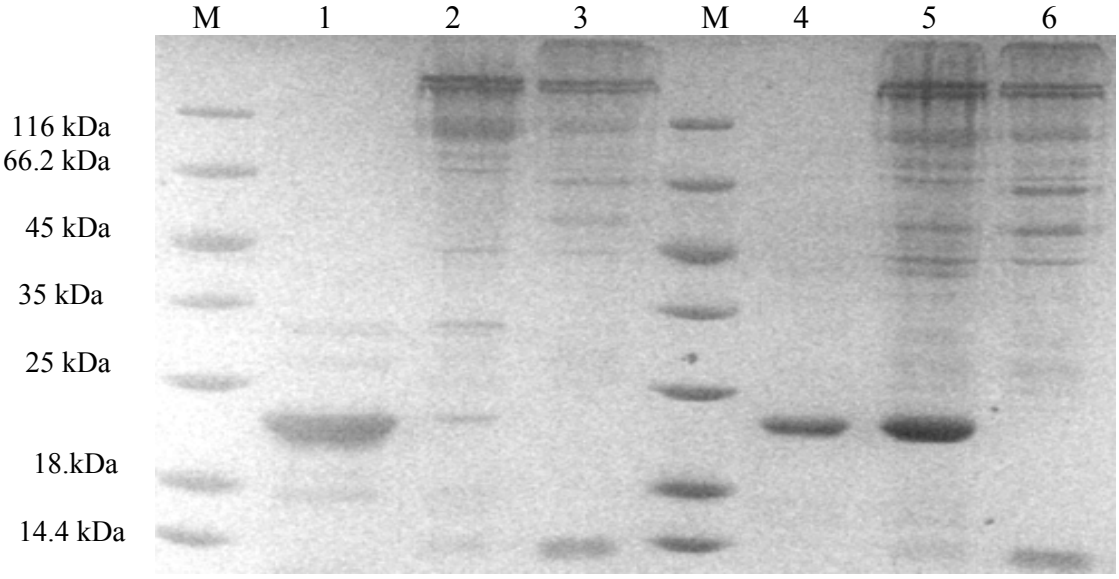

(B)

Figure 3. 6: Binding of CAMP factor fragments to sphingomyelinase-treated sheep erythrocyte membranes. (A) Lane M, protein marker; Lane 1, $CAMP^{114-226}$; Lane 2, $CAMP^{114-226}$ incubated with cell membranes; Lane 3, cell membranes without CAMP factor protein; Lane 4, $CAMP^{1-113}$; Lane 5, $CAMP^{1-113}$ incubated with cell membranes. (B) Lane M, protein marker; Lane 1, $CAMP^{1-170}$; Lane 2, $CAMP^{1-170}$ incubated with cell membranes; Lane 3 and 6, cell membranes without CAMP factor protein; Lane 4, $CAMP^{57-226}$; Lane 5, $CAMP^{57-226}$ incubated with cell membranes

Due to the small size of CAMP$^{1-56}$ and to interference by erythrocyte membrane proteins, its binding could not be reliably assessed by SDS-PAGE. Therefore, the binding was analyzed by spectrofluorimetry. To this end, one amino acid from CAMP$^{1-56}$ (Serine54) was replaced with cysteine by site-specific mutagenesis, and the mutant cysteine was labelled by modification with fluorescein maleimide. The binding of labelled CAMP1-56 to membranes was then observed from fluorescence emission after incubation and removal of unbound fragments by centrifugation (Figure 3.7). The binding efficiency was determined by comparing this emission intensity with the emission intensity from fragment solution without incubation with membrane. CAMP$^{1-56}$ showed membrane-binding efficiency of 40.1 ± 1.1%. All the other fragments were also labelled and analyzed for binding efficiency: CAMP$^{57-226}$ (101.2 ± 3.1%), CAMP$^{1-113}$ (11.3 ± 0.8%), CAMP$^{114-226}$ (28.4 ± 0.8%), CAMP$^{1-170}$ (14.8 ± 0.7%), and CAMP$^{171-226}$ (32.5 ± 1.2%) (Appendix 2).

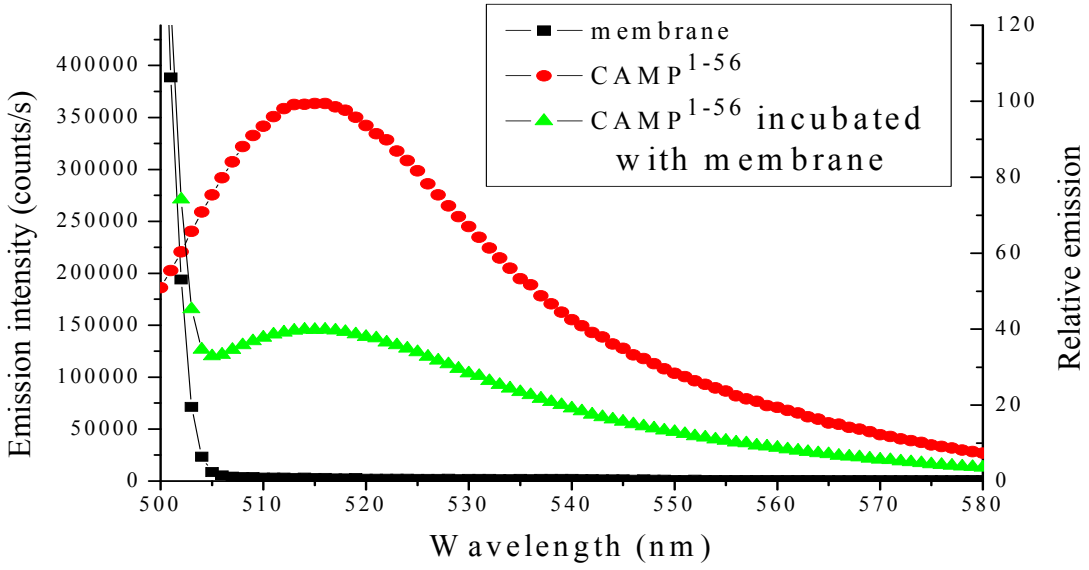

Figure 3.7: Fluorescence emission spectra of CAMP$^{1-56}$ (5µM) labelled with fluorescein maleimde with excitation at 492 nm.

3.5 Hemolytic inhibition by CAMP factor fragments

For PFTs, after binding to membranes, oligomerization is required before the pore-formation. Both CAMP$^{1-56}$ and CAMP$^{114-226}$ showed the ability of binding to membrane, but neither of them has hemolytic activity. To determine their ability to oligomerize, chemical cross-linking assays were performed on liposomes, but there was no oligomer observed for either of them. This suggested that CAMP$^{1-56}$ and CAMP$^{114-226}$ lost their ability of oligomerize. Presumably, oligomerization involves two complementary surfaces of molecules (Figure 3.8). The loss of oligomerization could be the consequence of two possiblities: (1) Inactivation of both oligomerization surfaces; (2) loss of only one side. As shown in Figure 3.8 A, in the latter case the fragment molecules cannot oligomerize to each other; but when they are incubated with intact proteins, they could associate to them on one side and thereby stop the further oligomerization (Figure 3.8 B). This, in turn, should result in an inhibition of the activity of the intact toxin.

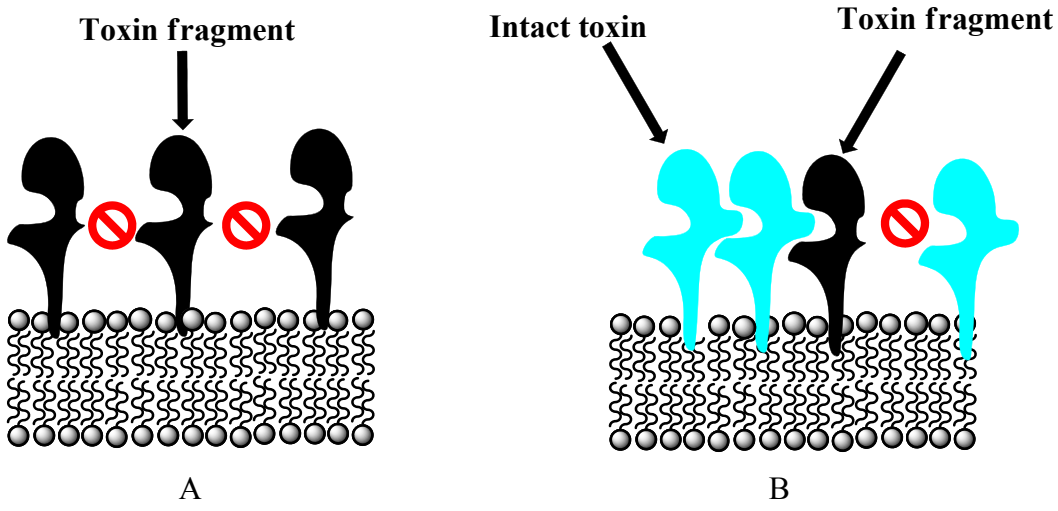

Figure 3. 8 Schematic representation of oligomerization inhibition.
A, fragments cannot oligomerize each other even if only one oligomerization surface is inactivated. B, fragments that have lost one oligomerization surface may inhibit the oligomerization of intact protein molecules.

To detect if fragments lost all of their olgomerization ability, the hemolytic activities of complete CAMP factor incubated with each of them were measured. The time required by CAMP factor (1μg/mL) to reach 50% hemolysis of 0.5% (v/v) sphingomyelinase-treated cells was increased from 15 minutes to 30 minutes with addition of $CAMP^{114-226}$ at a concentration of 16μg/mL (Figure 3.7). This suggested that, $CAMP^{114-226}$ could oligomerize to one side of CAMP factor, which inhibits hemolysis. However, it did not rule out the possibility that $CAMP^{114-226}$ inhibits hemolysis by intact CAMP factor by competing for binding sites.

With further increasing concentrations of $CAMP^{114-226}$ (32 and 64 μg/mL), the hemolysis was not reduced further. This might due to the association of the fragment with intact CAMP factor being weak and reversible, and the second molecule of CAMP factor can dislodge the fragment and bind irreversibly. This would more or less account for the kinetics; when the fragment was at high enough concentration, the CAMP factor would initially saturate with fragment but then get rid of it by interacting with each other.

There was no hemolytic inhibition was observed with $CAMP^{1-56}$ even at a concentration up to 200 μg/mL, which suggested that it was not capable of competing membrane receptor and lost its oligomerization ability on both sides.

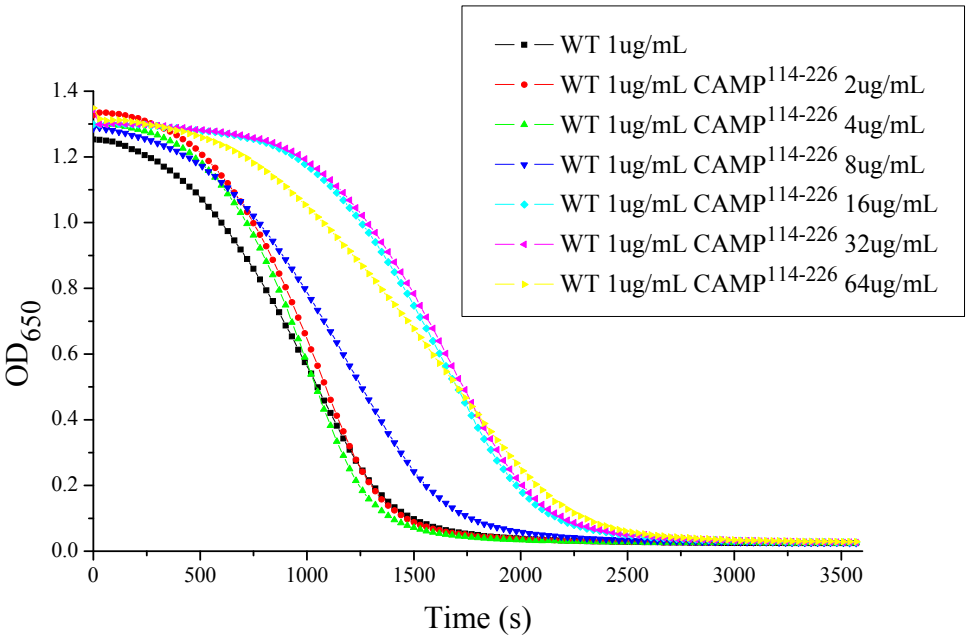

Figure 3. 9 Hemolytic titration of CAMP factor incubated with CAMP$^{114\text{-}226}$.

The 50% hemolysis was achieved by CAMP factor (1 µg/mL) in 15 minutes. With co-incubation of CAMP$^{114\text{-}226}$ at the concentration of 8 µg/mL, the 50% hemolysis was achieved in 20 minutes; with co-incubation of CAMP$^{114\text{-}226}$ at the concentration of 16, 32 and 64 µg/mL, the 50% hemolysis was achieved in 30 minutes. Sphingomyelinase-treated sheep erythrocytes (0.5% v/v) were used. The CAMP factor concentration was 1 µg/mL.

3.6 Membrane Binding competition

CAMP$^{114\text{-}226}$ inhibited the hemolysis of intact CAMP factor, though it is not clear if it was due to the competition for membrane receptor binding. In the binding competition assay, 1 µg/mL of labelled CAMP factor (F109C) was incubated with CAMP114-226 at concentrations of 4, 8, 16, and 32 µg/mL and sphingomyelinase-treated ghost membranes (equivalent to 0.5 %(v/v) blood cells). The fluorescein emission was recorded after all unbound proteins had been removed (Figure 3.10). With increasing concentrations of CAMP$^{114\text{-}226}$, the emission remained unchanged, indicating that binding was unaffected;

the reduced rate of hemolysis therefore must indeed be related to an inhibition of oligomerization rather than binding.

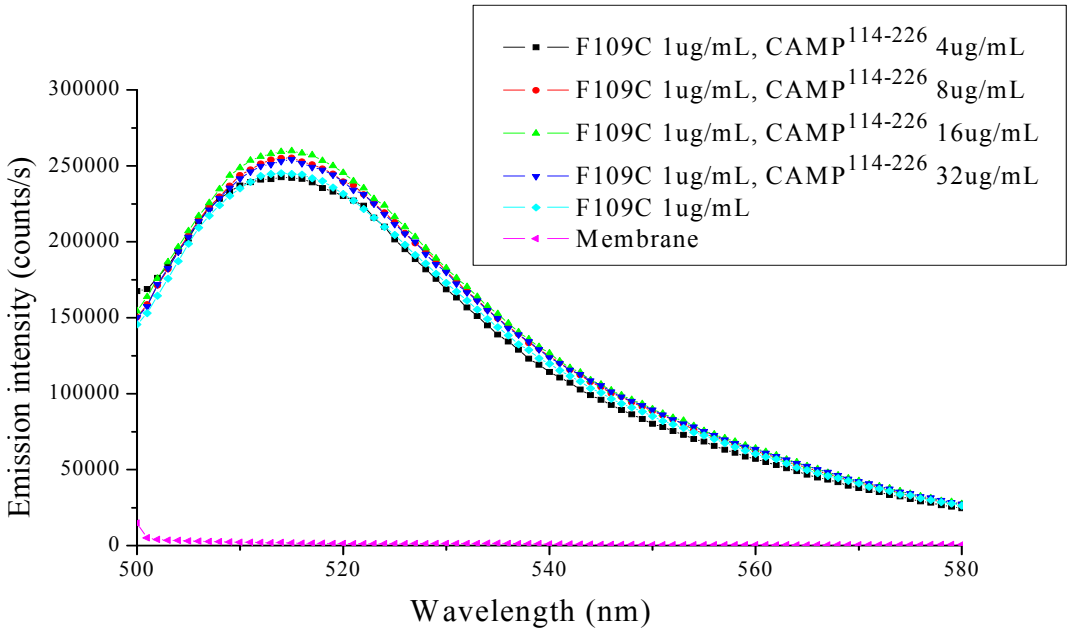

Figure 3. 10 Emission spectra of fluorescein labeled CAMP factor F109C.
It was incubated with CAMP114-226 at different concentrations for 20 minutes.

From the experiments done before, the general abilities of all the fragments are summarized in Table 3.2. The relative positions of CAMP factor fragments were compared with the transmembrane prediction plot obtained from the on-line program "DAS TM-segment prediction" at http://www.sbc.su.se/~miklos/DAS/ (Figure 3.11). The peak regions in the plot are the possible transmembrane regions. The region between 104 and 113 was previously identified as transmembrane region [*56, 63*].

Table 3. 2 The general abilities of CAMP factor fragments

Protein	Hemolysis	50% hemolysis	Membrane binding	Binding efficiency	Hemolytic inhibition	Binding competition
CAMP factor 	Yes	15 min at 1μg/mL	Yes	--	--	--
$CAMP^{1-56}$ 	No	--	Yes	40.1±1.1%	No	--
$CAMP^{1-113}$ 	Yes	30 min at 400μg/mL	Yes	11.3±0.8%	--	--
$CAMP^{1-170}$ 	Yes	15 min at 100μg/mL	Yes	14.8±0.7%	--	--
$CAMP^{171-226}$ 	Yes	10 min at 400μg/mL	Yes	32.5±1.2%	--	--
$CAMP^{114-226}$ 	No	--	Yes	28.4±0.8%	Yes	No
$CAMP^{57-226}$ 	Yes	15 min at 12.5μg/mL	Yes	101.2±3.1%	--	--

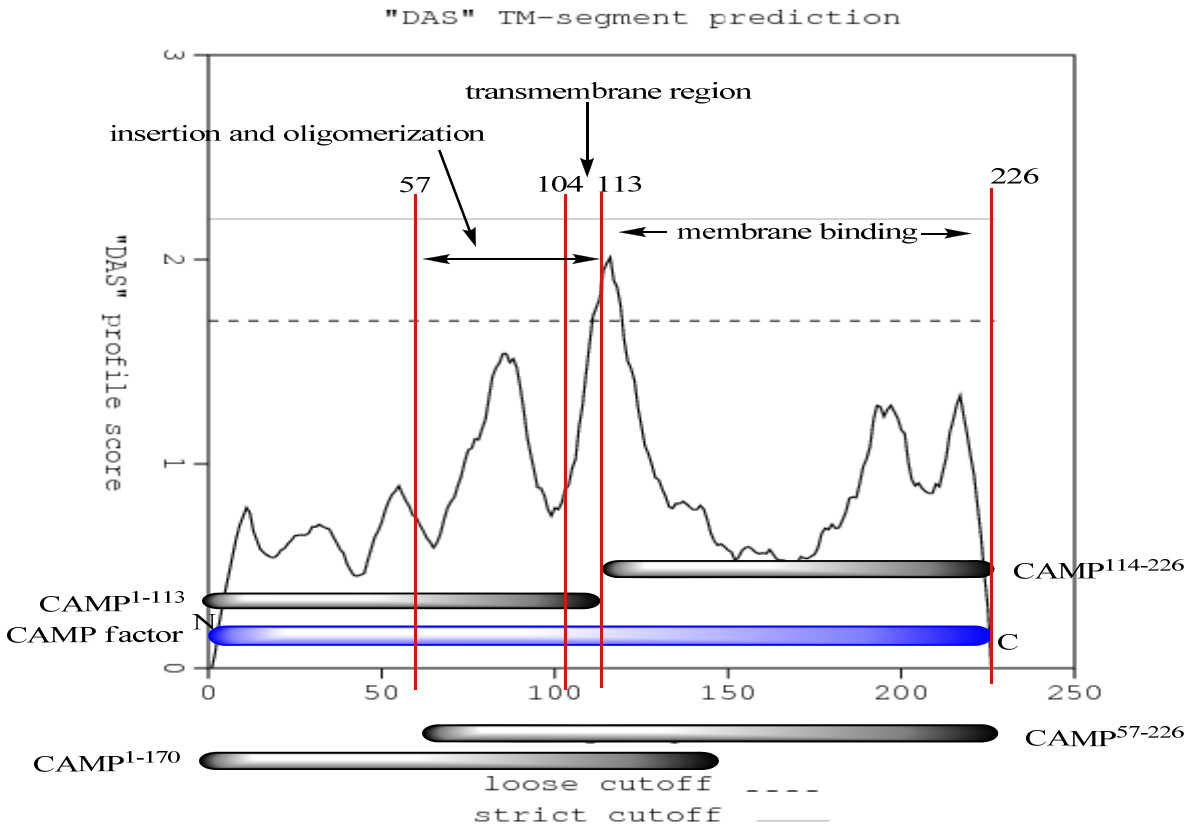

Figure 3. 11 Relative positions of CAMP factor fragments.

The relative positions of the CAMP factor fragments were compared with a CAMP factor transmembrane prediction graph. The previously identified transmembrane region is labeled between 104 and 113.

3.7 Unknown protein

Before the CAMP$^{171-226}$ was purified under denaturing conditions, it was eluted with an unknown protein with a size of around 66 kDa, which was suspected as an octamer of CAMP$^{171-226}$. These two species were separated by gel filtration and analyzed by mass spectrometry (Figure 3.8). The possibility that the unknown protein might be an octamer was thereby eliminated. Nevertheless, the unknown protein was observed to have hemolytic activity to sphingomyeliase-treated sheep blood cells (Figure 3.12).

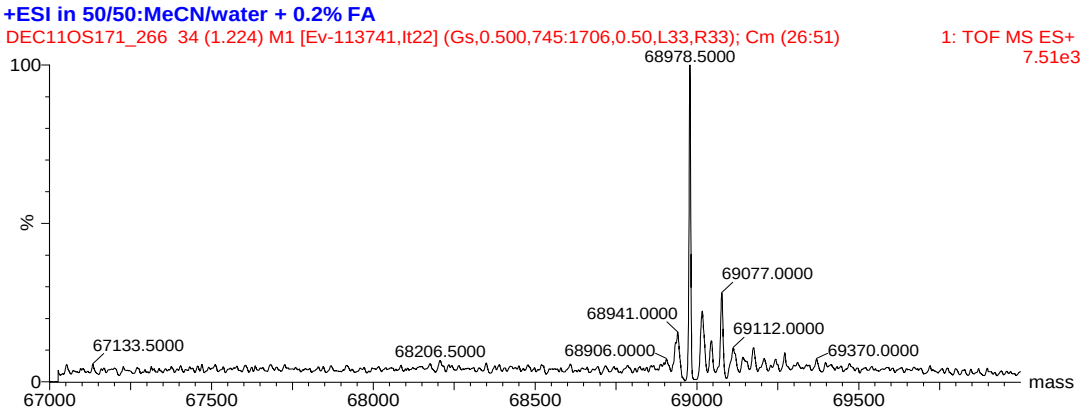

A

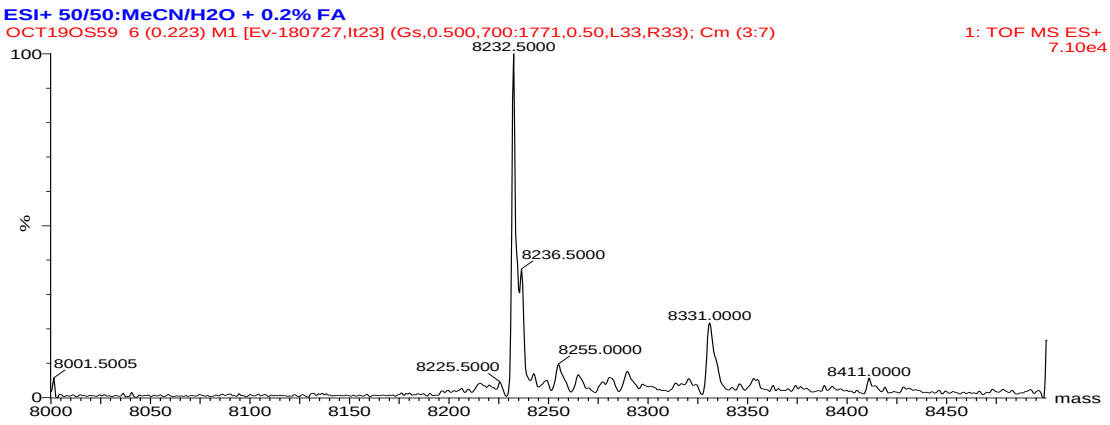

B

Figure 3. 12 Mass spectra of CAMP$^{171-226}$ and an unknown protein.

A. The unknown protein (68978.5 Da). B. CAMP$^{171-226}$ (8232 Da)

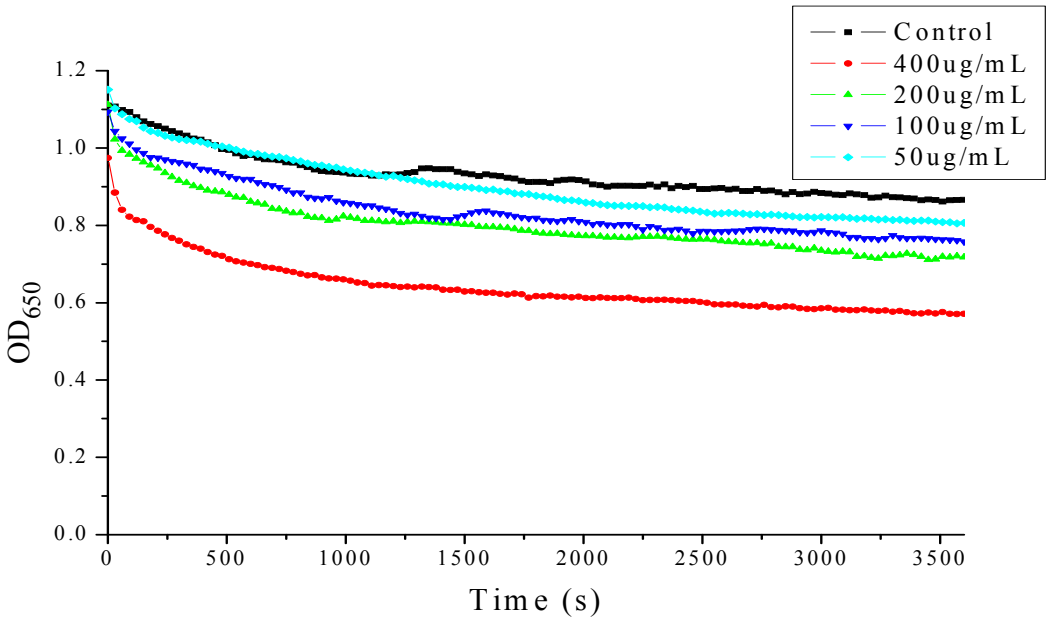

Figure 3. 13 Hemolytic titration of unknown 68kDa protein

3.8 Discussion

Streptococcus agalactiae CAMP factor, a membrane pore-forming toxin, is considered to have the same action mechanism as other PFTs: binding, oligomerization, and membrane insertion. With many PFTs, these functions reside in specific regions of the molecule. The studies on CAMP factor mutant ($CAMP^{W167F}$) done by our former lab member (Shanshan Liu) have shown that $CAMP^{W167F}$ could bind to sphingomyelinase-treated sheep erythrocyte membrane but suffered a significant loss in hemolytic activity [*56*]. This finding indicates that CAMP factor could have specific regions for the different stages during pore-formation.

To reveal the regions responsible for these functions, six CAMP factor fragments, $CAMP^{1-56}$, $CAMP^{57-226}$, $CAMP^{1-113}$, $CAMP^{114-226}$, $CAMP^{1-170}$, and $CAMP^{171-226}$, were constructed using site-specific mutagenesis. After protein purification, these fragments were all subject to hemolytic titration. Fragments $CAMP^{1-56}$ and $CAMP^{114-226}$ showed no hemolytic activity. The other fragments showed different levels of hemolytic activity. Among them, $CAMP^{57-226}$ and $CAMP^{1-170}$ showed the strongest activity; they could achieve 50% hemolysis in 15 minutes at a concentration of 12.5 μg/mL and 100 μg/mL respectively.

From this activity comparison, the most active fragments have sequence overlapping between residues 57 and 170. A little activity was shown in fragment $CAMP^{1-113}$, so residues 57-113 seem to be absolutely essential; adjoining regions, particularly those at the C-terminus, contribute a lot.

From hydrophobicity predictions, this region contains the most likely membrane inserted regions. From the cysteine-scanning mutagenesis studies done by Shanshan Liu

and David Donkor, this region is involved in membrane insertion [*56, 63*]. This probably explained the much higher activity for CAMP$^{1-170}$ and CAMP$^{57-226.}$

Fragments CAMP$^{1-56}$ and CAMP$^{114-226}$, that do not show activity, were shown to be able to bind to cell membranes. The membrane binding could be examined using SDS-PAGE, however, the interference caused by membrane proteins could be very strong, particularly for small fragments and fragments with low binding efficiency. By using fluorometric method, the membrane binding efficiency was quantitatively measured with fluorescein-labelled fragments. The membrane binding efficiency of the haemolytically inactive CAMP$^{114-226}$ (28.4±0.8%) was shown to be even higher than that of the slightly active CAMP$^{1-113}$ (11.3±0.8%). These binding results suggested these two fragment are lacking either oligomerization or insertion ability. Chemical cross-linking assay was performed on both fragments, however, neither of them showed oligomerization.

Within an oligomer of rotational symmetry, each subunit must expose two distinct and contact surfaces that interact with the complemenrary surfaces on neighbouring subunits. In a fragment that has lost the ability to oligomerize, either or both contact surfaces may be affected. If only one surface were affected, the fragment should still be able to associate with intact proteins one side and thereby inhibit the further progress of oligomerization and therefore hemolysis.

Both CAMP$^{1-56}$ and CAMP$^{114-226}$ were assayed for their ability of inhibiting hemolysis of CAMP factor. CAMP$^{1-56}$ did not show any inhibition of hemolysis. In contrast, CAMP$^{114-226}$ showed inhibition that increased up to a concentration of 16μg/mL. Beyond that concentration, the extent of inhibition levelled off.

The inhibition of hemolysis observed with $CAMP^{114-226}$ might be caused by oligomerization termination or, alternatively, by competition for membrane receptors. The membrane binding competition was assayed, which ruled out the second possibility.

Inhibition levelled off beyond the concentration of 16μg/mL could be caused by the weak interaction between fragement and intact protein. When the fragment concentration was higher than 16μg/mL, all the intact CAMP factor protein was associated with the fragments, which gave the saturated inhibition level. The interaction between intact CAMP factor is stronger, which allows the fragment-associated CAMP factor to oligomerize each other after dislodging the fragment.

The weak hemolytic activity from $CAMP^{171-226}$ was unexpected comparing to hemolytic inactive $CAMP^{114-226}$.

All the fragments were shown to have membrane binding ability and their binding efficiency were measured; the binding efficiency of the hemolytic inactive fragments $CAMP^{1-56}$ (40.1±1.1%) and $CAMP^{114-226}$ (28.4±0.8%) are higher than the hemolytic fragments $CAMP^{1-170}$ (14.8.±0.7%) and $CAMP^{1-113}$ (11.3±0.8%). Therefore the binding ability resides in a region that separated from those for oligomerization and insertion. Among the hemolytic fragments, the more active fragments also showed higher membrane binding efficiency.

From this study, CAMP factor is shown again to have conserved regions for different functions. The region between residues 57 and 113 in CAMP factor is critical for completing hemolysis, which is involved in membrane insertion. The fragments lacking this region have partial or no oligomerizing ability, suggested that it was also responsible

for complete oligomerization. The high binding efficiency of CAMP$^{114-226}$ showed that the major binding domain resides in this region.

3.9 Future studies

To elucidate the detailed information about the regions responsible for all the action stages, more CAMP factor fragments could be obtained by the same method and assayed for their ability.

For the hemolytic fragments, they will be tested for their activity on liposomes enclosing calcein. The pores formed by these fragments will be studied by osmotic protection by PEG, and electron microscopy to compare with CAMP factor.

CAMP factor has been shown to bind to GPI-anchored protein [*22, 64*], the further investigation on this binding interaction could be done with the aid of CAMP factor fragments.

References

(1) Alouf JE, F. J. (1999) *The comprehensive sourcebook of bacterial protein toxins*, Academic, London.

(2) Goot, F. G. v. d. (2001) *Pore-forming toxins*, Vol.257, Spriger, New York, N.Y.

(3) Macfarlane, M. G., and Knight, B. C. (1941) The biochemistry of bacterial toxins: The lecithinase activity of Cl. welchii toxins. *Biochem J 35*, 884-902.

(4) Dhople, V. M., and Nagaraj, R. (1993) Delta-toxin, unlike melittin, has only hemolytic activity and no antimicrobial activity: rationalization of this specific biological activity. *Biosci Rep 13*, 245-50.

(5) Ladokhin, A. S., and White, S. H. (2001) 'Detergent-like' permeabilization of anionic lipid vesicles by melittin. *Biochim Biophys Acta 1514*, 253-60.

(6) Alouf, J. E., Dufourcq, J., Siffert, O., Thiaudiere, E., and Geoffroy, C. (1989) Interaction of staphylococcal delta-toxin and synthetic analogues with erythrocytes and phospholipid vesicles. Biological and physical properties of the amphipathic peptides. *Eur J Biochem 183*, 381-90.

(7) Shai, Y. (1999) Mechanism of the binding, insertion and destabilization of phospholipid bilayer membranes by alpha-helical antimicrobial and cell non-selective membrane-lytic peptides. *Biochim Biophys Acta 1462*, 55-70.

(8) Anderluh, G., Barlic, A., Podlesek, Z., Macek, P., Pungercar, J., Gubensek, F., Zecchini, M. L., Serra, M. D., and Menestrina, G. (1999) Cysteine-scanning mutagenesis of an eukaryotic pore-forming toxin from sea anemone: topology in lipid membranes. *Eur J Biochem 263*, 128-36.

(9) Janeway, C. A., Travers, P., Walport, M., and Shlomchik, M.J. (2005) *Immuno biology*, 6th ed., Garland Science Publishing, New York.

(10) Jurgens, D., Shalaby, F. Y., and Fehrenbach, F. J. (1985) Purification and characterization of cAMP-factor from Streptococcus agalactiae by hydrophobic interaction chromatography and chromatofocusing. *J Chromatogr 348*, 363-70.

(11) Lang, S., and Palmer, M. (2003) Characterization of Streptococcus agalactiae CAMP factor as a pore-forming toxin. *J Biol Chem 278*, 38167-73.

(12) Roh, J. Y., Choi, J. Y., Li, M. S., Jin, B. R., and Je, Y. H. (2007) Bacillus thuringiensis as a specific, safe, and effective tool for insect pest control. *J Microbiol Biotechnol 17*, 547-59.

(13) Schnepf, E., Crickmore, N., Van Rie, J., Lereclus, D., Baum, J., Feitelson, J., Zeigler, D. R., and Dean, D. H. (1998) Bacillus thuringiensis and its pesticidal crystal proteins. *Microbiol Mol Biol Rev 62*, 775-806.

(14) Bechinger, B., and Lohner, K. (2006) Detergent-like actions of linear amphipathic cationic antimicrobial peptides. *Biochim Biophys Acta 1758*, 1529-39.

(15) Bulet, P., and Stocklin, R. (2005) Insect antimicrobial peptides: structures, properties and gene regulation. *Protein Pept Lett 12*, 3-11.

(16) Raghuraman, H., and Chattopadhyay, A. (2007) Melittin: a membrane-active peptide with diverse functions. *Biosci Rep 27*, 189-223.

(17) Zhai, Y., and Saier, M. H., Jr. (2000) The amoebapore superfamily. *Biochim Biophys Acta 1469*, 87-99.

(18) Woolley, G. A. (2007) Channel-forming activity of alamethicin: effects of covalent tethering. *Chem Biodivers 4*, 1323-37.
(19) Alouf, J. E. (2000) Cholesterol-binding cytolytic protein toxins. *Int J Med Microbiol 290*, 351-6.
(20) Palmer, M. (2001) The family of thiol-activated, cholesterol-binding cytolysins. *Toxicon 39*, 1681-9.
(21) Fivaz, M., Abrami, L., Tsitrin, Y., and van der Goot, F. G. (2001) Not as simple as just punching a hole. *Toxicon 39*, 1637-45.
(22) Lang, S., Xue, J., Guo, Z., and Palmer, M. (2007) Streptococcus agalactiae CAMP factor binds to GPI-anchored proteins. *Med Microbiol Immunol 196*, 1-10.
(23) Bhakdi, S., and Tranum-Jensen, J. (1988) Damage to cell membranes by pore-forming bacterial cytolysins. *Prog Allergy 40*, 1-43.
(24) Bhakdi, S., and Tranum-Jensen, J. (1991) Alpha-toxin of Staphylococcus aureus. *Microbiol Rev 55*, 733-51.
(25) Valeva, A., Pongs, J., Bhakdi, S., and Palmer, M. (1997) Staphylococcal alpha-toxin: the role of the N-terminus in formation of the heptameric pore -- a fluorescence study. *Biochim Biophys Acta 1325*, 281-6.
(26) Gilbert, R. J., Jimenez, J. L., Chen, S., Andrew, P. W., and Saibil, H. R. (2000) Structural basis of pore formation by cholesterol-binding toxins. *Int J Med Microbiol 290*, 389-94.
(27) Shatursky, O., Heuck, A. P., Shepard, L. A., Rossjohn, J., Parker, M. W., Johnson, A. E., and Tweten, R. K. (1999) The mechanism of membrane insertion for a cholesterol-dependent cytolysin: a novel paradigm for pore-forming toxins. *Cell 99*, 293-9.
(28) Chakraborty, T., Huhle, B., Hof, H., Bergbauer, H., and Goebel, W. (1987) Marker exchange mutagenesis of the aerolysin determinant in Aeromonas hydrophila demonstrates the role of aerolysin in A. hydrophila-associated systemic infections. *Infect Immun 55*, 2274-80.
(29) Collier, R. J., and Young, J. A. (2003) Anthrax toxin. *Annu Rev Cell Dev Biol 19*, 45-70.
(30) Mitchell, T. J., Andrew, P. W., Saunders, F. K., Smith, A. N., and Boulnois, G. J. (1991) Complement activation and antibody binding by pneumolysin via a region of the toxin homologous to a human acute-phase protein. *Mol Microbiol 5*, 1883-8.
(31) Portnoy, D. A., Chakraborty, T., Goebel, W., and Cossart, P. (1992) Molecular determinants of Listeria monocytogenes pathogenesis. *Infect Immun 60*, 1263-7.
(32) Sato, N., Kurotaki, H., Watanabe, T., Mikami, T., and Matsumoto, T. (1998) Use of hemoglobin as an iron source by *Bacillus cereus*. *Biol Pharm Bull 21*, 311-4.
(33) Burns, D. L. (2003) *Bacterial protein toxins*, ASM Press, Washington, D.C.
(34) Cabiaux, V., Wolff, C., and Ruysschaert, J. M. (1997) Interaction with a lipid membrane: a key step in bacterial toxins virulence. *Int J Biol Macromol 21*, 285-98.
(35) Walker, B., Krishnasastry, M., Zorn, L., Kasianowicz, J., and Bayley, H. (1992) Functional expression of the alpha-hemolysin of Staphylococcus aureus in intact Escherichia coli and in cell lysates. Deletion of five C-terminal amino acids selectively impairs hemolytic activity. *J Biol Chem 267*, 10902-9.

(36) Olson, R., Nariya, H., Yokota, K., Kamio, Y., and Gouaux, E. (1999) Crystal structure of staphylococcal LukF delineates conformational changes accompanying formation of a transmembrane channel. *Nat Struct Biol 6*, 134-40.
(37) Song, L., Hobaugh, M. R., Shustak, C., Cheley, S., Bayley, H., and Gouaux, J. E. (1996) Structure of staphylococcal alpha-hemolysin, a heptameric transmembrane pore. *Science 274*, 1859-66.
(38) Montoya, M., and Gouaux, E. (2003) Beta-barrel membrane protein folding and structure viewed through the lens of alpha-hemolysin. *Biochim Biophys Acta 1609*, 19-27.
(39) Palmer, M., Saweljew, P., Vulicevic, I., Valeva, A., Kehoe, M., and Bhakdi, S. (1996) Membrane-penetrating domain of streptolysin O identified by cysteine scanning mutagenesis. *J Biol Chem 271*, 26664-7.
(40) Shepard, L. A., Shatursky, O., Johnson, A. E., and Tweten, R. K. (2000) The mechanism of pore assembly for a cholesterol-dependent cytolysin: formation of a large prepore complex precedes the insertion of the transmembrane beta-hairpins. *Biochemistry 39*, 10284-93.
(41) Ramachandran, R., Tweten, R. K., and Johnson, A. E. (2004) Membrane-dependent conformational changes initiate cholesterol-dependent cytolysin oligomerization and intersubunit beta-strand alignment. *Nat Struct Mol Biol 11*, 697-705.
(42) Ramachandran, R., Heuck, A. P., Tweten, R. K., and Johnson, A. E. (2002) Structural insights into the membrane-anchoring mechanism of a cholesterol-dependent cytolysin. *Nat Struct Biol 9*, 823-7.
(43) Bernheimer, A. W., Linder, R., and Avigad, L. S. (1979) Nature and mechanism of action of the CAMP protein of group B streptococci. *Infect Immun 23*, 838-44.
(44) Christie R, A. N., Munch-Petersen E. (1944) A note on a lytic phenomenon shown by group B streptococci. *Aust J Exp Biol 22*, 197-200.
(45) McKellar, R. C. (1994) Use of the CAMP test for identification of Listeria monocytogenes. *Appl Environ Microbiol 60*, 4219-25.
(46) Munch-Petersen E, a. R. C. (1947) On the effect of the interaction of staphylococcal beta-toxin and group B streptococcal substance on red blood corpuscles and its use as a test for the identification of Streptococcus agalactiae. *J Pathol Bacteriol 59*, 367.
(47) Darling, C. L. (1975) Standardization and evaluation of the CAMP reaction for the prompt, presumptive identification of Streptococcus agalactiae (Lancefield group B) in clinical material. *J Clin Microbiol 1*, 171-4.
(48) Lindquist, J. (2004) Differential Media: Hemolytic Reactions and the CAMP Test http://www.jlindquist.net/generalmicro/dfhemo.html.
(49) Sterzik, B., and Fehrenbach, F. J. (1985) Reaction components influencing CAMP factor induced lysis. *J Gen Microbiol 131*, 817-20.
(50) Nelson, G. J. (1967) Lipid composition of erythrocytes in various mammalian species. *Biochim Biophys Acta 144*, 221-32.
(51) Fehrenbach, F. J., Sterzik, B., Schmidt, C.M., and Jurgens, D. (1984) Interaction of the CAMP-factor from *S.agalactiae* with artificial membranes. *Bacterial Protein Toxins*, 317-324.

(52) Brown, J., Farnsworth, R., Wannamaker, L. W., and Johnson, D. W. (1974) CAMP factor of group B streptococci: production, assay, and neutralization by sera from immunized rabbits and experimentally infected cows. *Infect Immun 9*, 377-83.
(53) Jurgens, D., Sterzik, B., and Fehrenbach, F. J. (1987) Unspecific binding of group B streptococcal cocytolysin (CAMP factor) to immunoglobulins and its possible role in pathogenicity. *J Exp Med 165*, 720-32.
(54) Hensler, M. E., Quach, D., Hsieh, C. J., Doran, K. S., and Nizet, V. (2008) CAMP factor is not essential for systemic virulence of Group B Streptococcus. *Microb Pathog 44*, 84-8.
(55) El-Huneidi, W., Mui, R., Zhang, T. H., and Palmer, M. (2007) Streptococcus agalactiae CAMP factor/protein B does not bind to human IgG. *Med Microbiol Immunol 196*, 73-7.
(56) Liu, S.,(2005) Identification of a membrane-spanning domain of Streptococcus agalactiae CAMP factor by cysteine scanning mutagenesis, MSc thesis in Chemistry University of Waterloo Waterloo, ON
(57) Howorka, S., and Bayley, H. (1998) Improved protocol for high-throughput cysteine scanning mutagenesis. *Biotechniques 25*, 764-6, 768, 770 passim.
(58) Ausubel, F. M. (1999) *Short protocols in molecular biology*, 4th ed., John Wiley & Sons, Inc., Toronto.
(59) Lang, S.,(2005) Funtional characterization of *streptococcus agalactiae* CAMP factor, and dual targeted labelling of proteins using cysteine and selenomethionine residues Chemistry University of Waterloo Waterloo
(60) Bradford, M. M. (1976) A rapid and sensitive method for the quantitation of microgram quantities of protein utilizing the principle of protein-dye binding. *Anal Biochem 72*, 248-54.
(61) Guan, K. L., and Dixon, J. E. (1991) Eukaryotic proteins expressed in Escherichia coli: an improved thrombin cleavage and purification procedure of fusion proteins with glutathione S-transferase. *Anal Biochem 192*, 262-7.
(62) Lundbald, R. L. (2000) *Techniques in protein modification*, CRC press.
(63) Donkor, D.,(2007) Membrane interaction of *streptococcus agalactiae* CAMP factor. MSc thesis in Chemistry University of Waterloo Waterloo, ON
(64) Wu, X., Shen, Z., Zeng, X., Lang, S., Palmer, M., and Guo, Z. (2008) Synthesis and biological evaluation of sperm CD52 GPI anchor and related derivatives as binding receptors of pore-forming CAMP factor. *Carbohydr Res 343*, 1718-29.

Appendices

A 1: Hemolytic titration of CAMP factor fragments

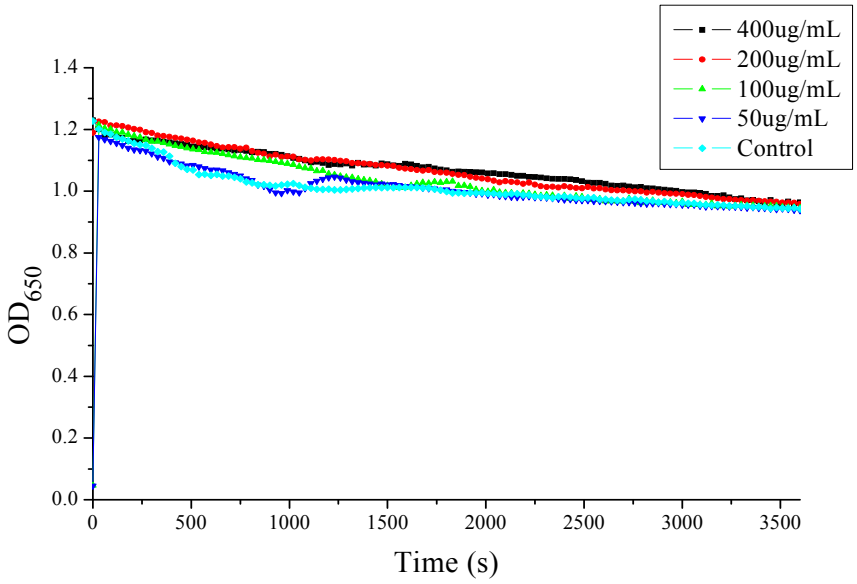

CAMP$^{1\text{-}56}$

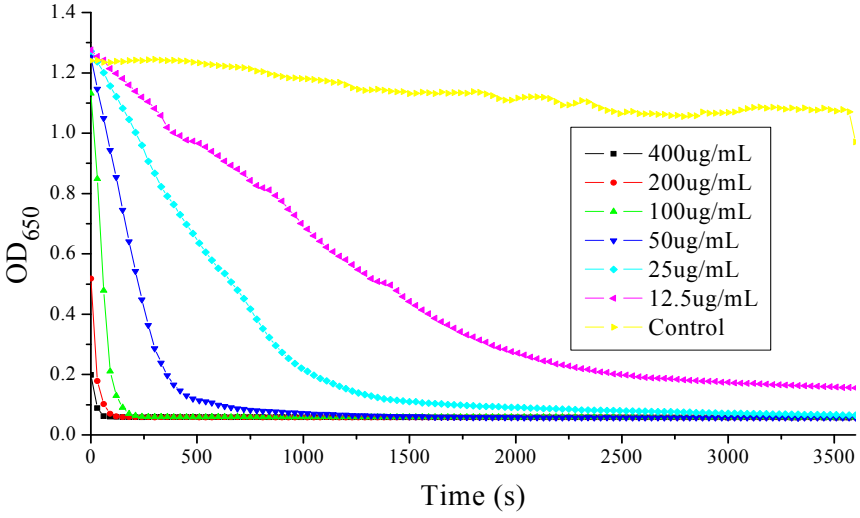

CAMP$^{57\text{-}226}$

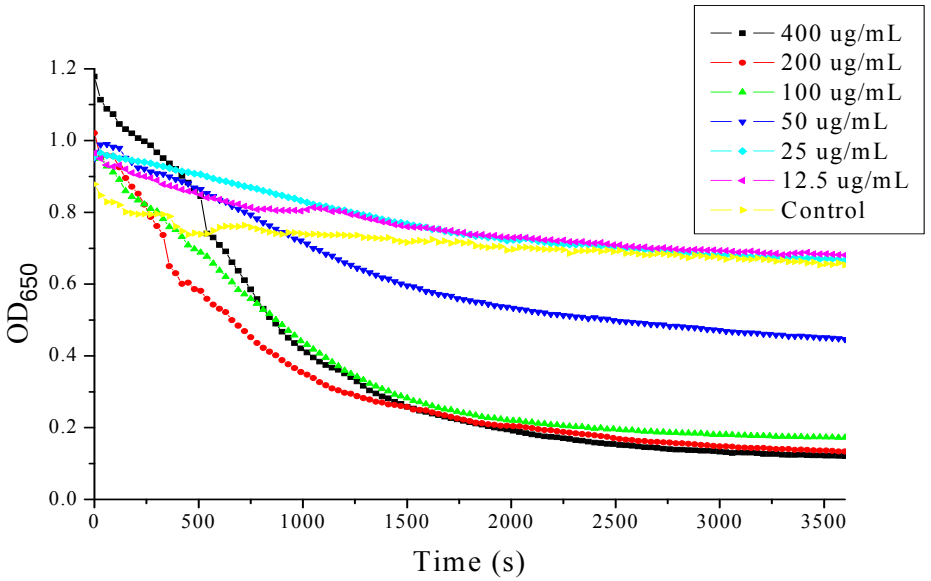

CAMP$^{1\text{-}170}$

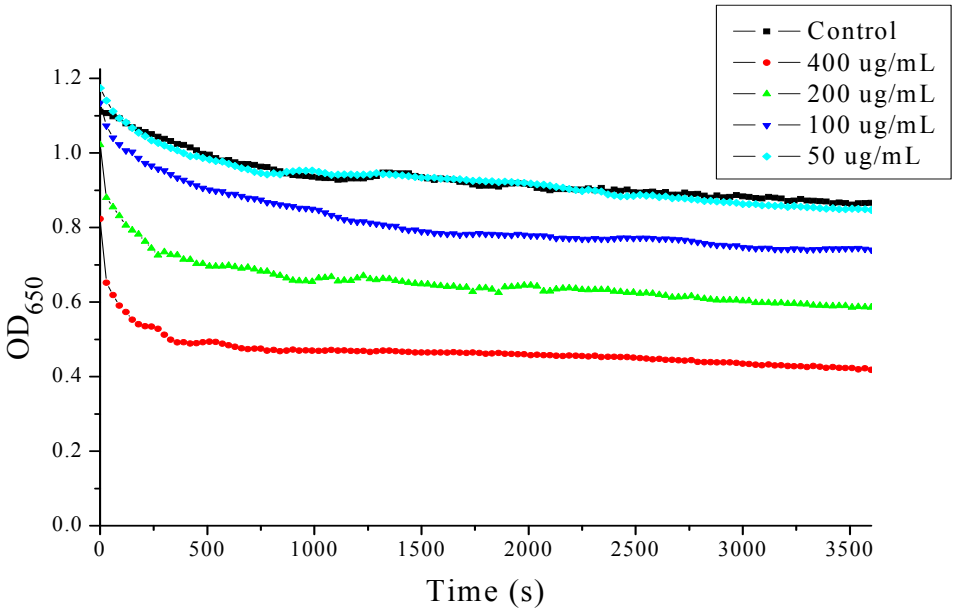

CAMP$^{171\text{-}226}$

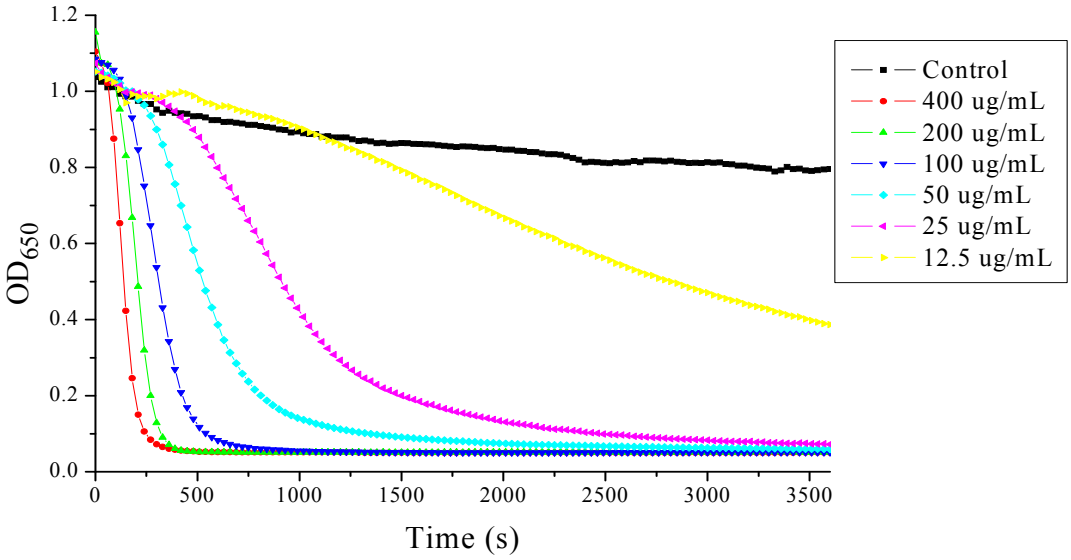

Hemolytic titration of protein mixture ($CAMP^{171-226}$, unknown 68kDa protein)

A 2: Membrane binding of CAMP factor fragment

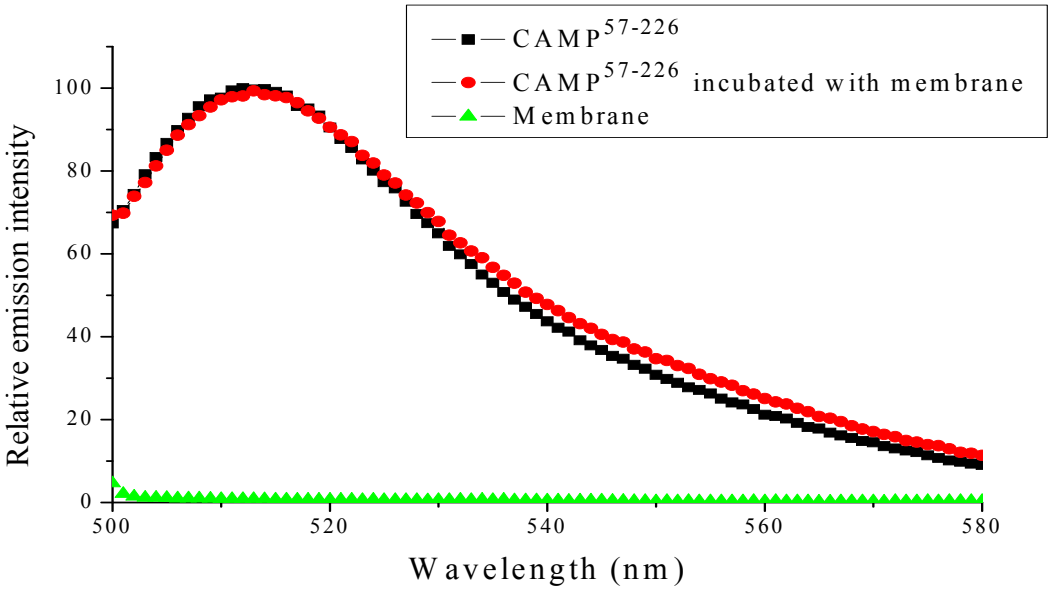

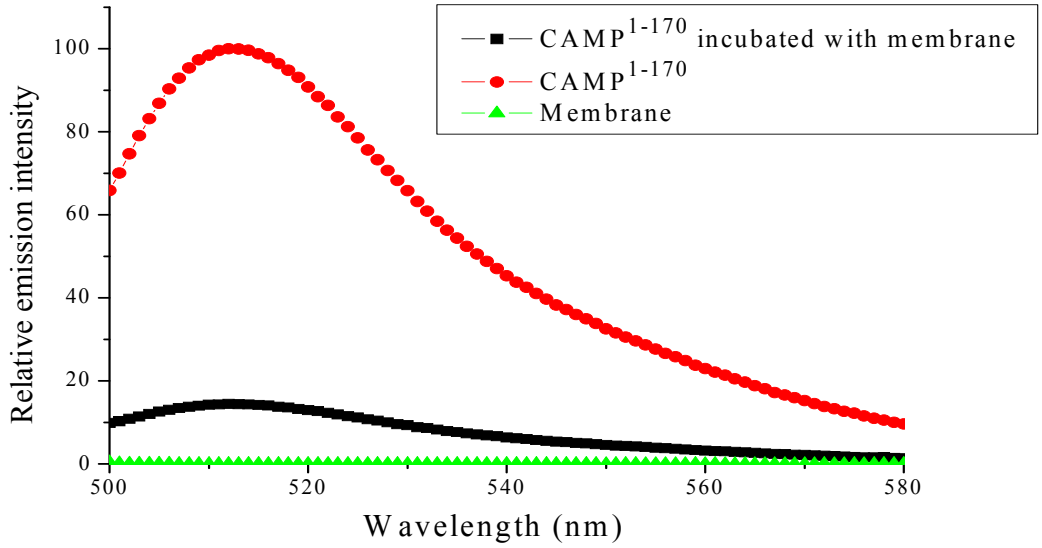

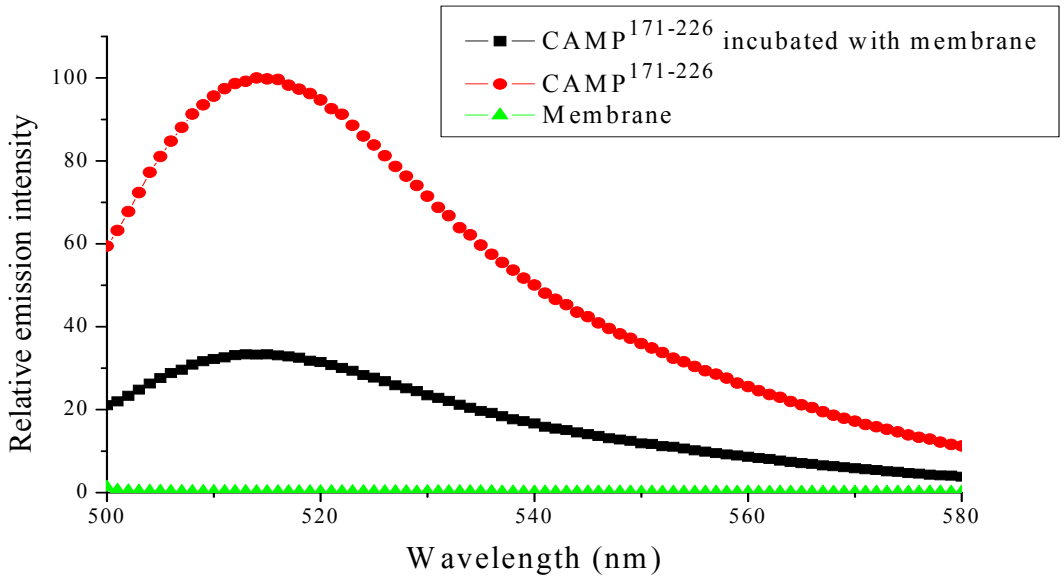
CAMP171-226 incubated with membrane
CAMP171-226
Membrane
Relative emission intensity
0
20
40
60
80
100
500
520
540
560
580
Wavelength (nm)

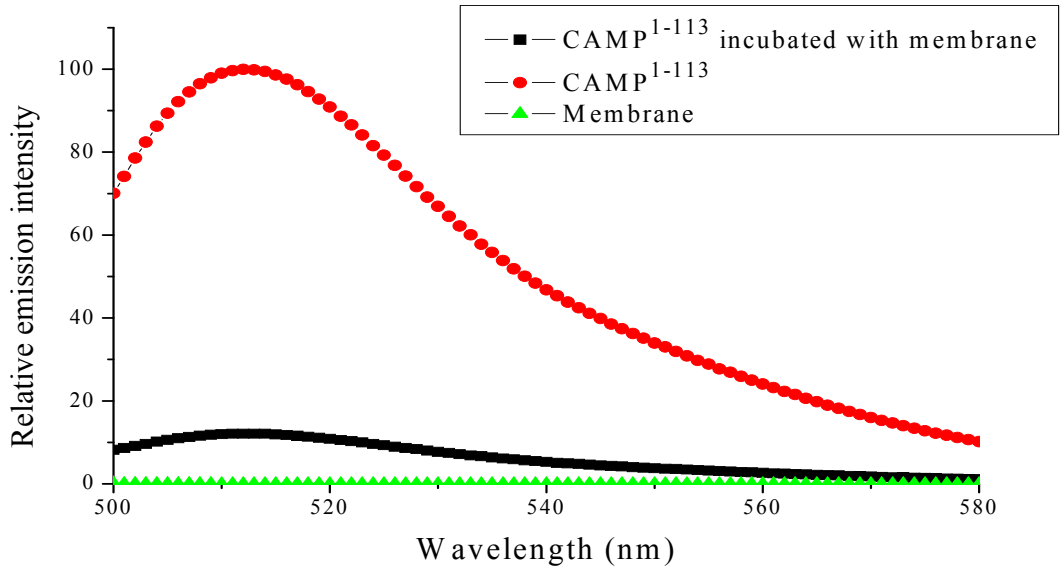
CAMP1-113 incubated with membrane
CAMP1-113
Membrane
Relative emission intensity
0
20
40
60
80
100
500
520
540
560
580
Wavelength (nm)

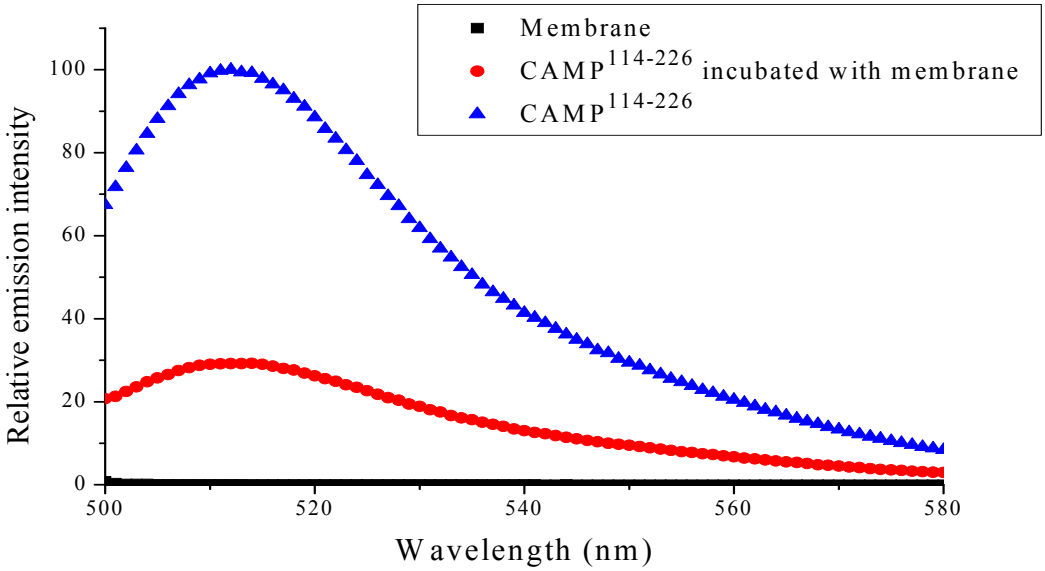
Membrane
CAMP114-226 incubated with membrane
CAMP114-226
Relative emission intensity
0
20
40
60
80
100
500
520
540
560
580
Wavelength (nm)